



Mechanism of electron multipacting with long bunched proton beam

— Theory and Simulation

L. Wang, BNL

In collaboration with J. Wei, M. Blaskiewicz, P. He, Y.Y Lee, D. Raparia, S.Y. Zhang (BNL), R. Macek (LANL), K. Ohmi (KEK), F. Zimmermann (CERN), A. Chao (SLAC)

The 13th ICFA Beam Dynamics Mini-Workshop
Beam Induced Pressure Rise in Rings
Brookhaven National Laboratory, Upton, NY
December 9 - 12, 2003

Content



- Motivation
- Electron motion in beam space charge field & Mechanism of trailing edge multipacting
- Important factors related to Multipacting
 - Longitudinal beam profile
 - Transverse beam shape & size
 - Beam intensity
 - Chamber size
 - Beam in gap
 - Peak SEY and Energy at Peak SEY
 -
- Electron cloud in dipole magnets & Quadrupole & Sextupole magnets
- Electron cloud clearing with solenoids & clearing electrodes
- Summary

Motivation

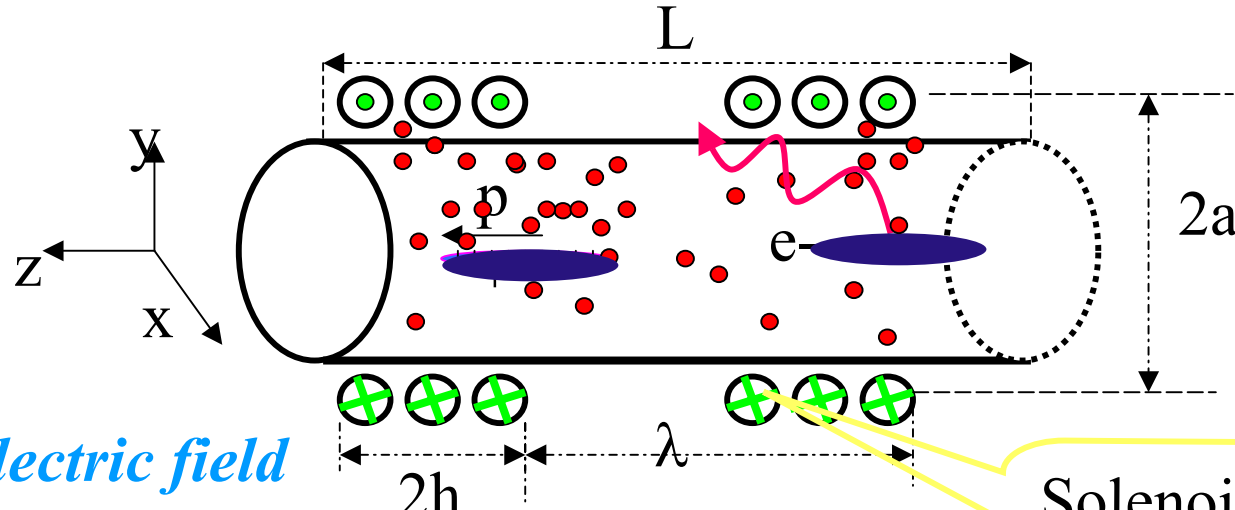


- What is the mechanism of trailing edge multipacting?
- Which factors affect e-cloud multipacting?
And How?
- How to Clear electron cloud?
- Why e-cloud is important in some accelerators,
but not in others?

CLOUDLAND is a complete 3D PIC code for e-cloud initially developed for KEKB (*PRST-AB 124402*)

Program model

- ♦ PIC methods



Magnetic and electric field

- ♦ General 3-dimensional fields given by expression.
- ♦ Fields can also be import from other program using table

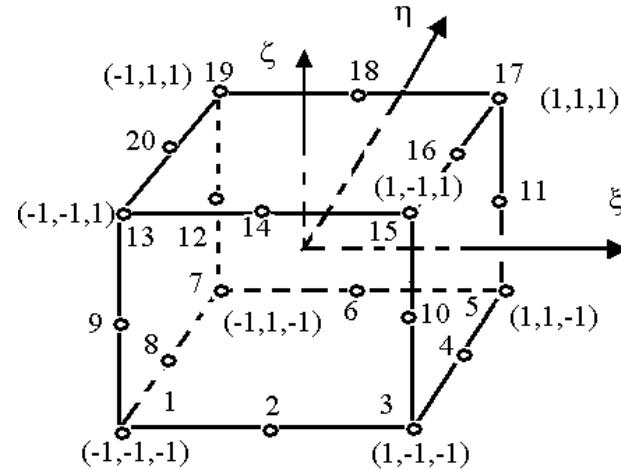
Beam potential

- ♦ Gaussian bunch in round chamber (image charge is included)
- ♦ PIC method for general geometry

Secondary emission and reflective electron are included

- Three dimensional irregular mesh to better represent the general chamber geometry

- handle accuracy with high order elements.



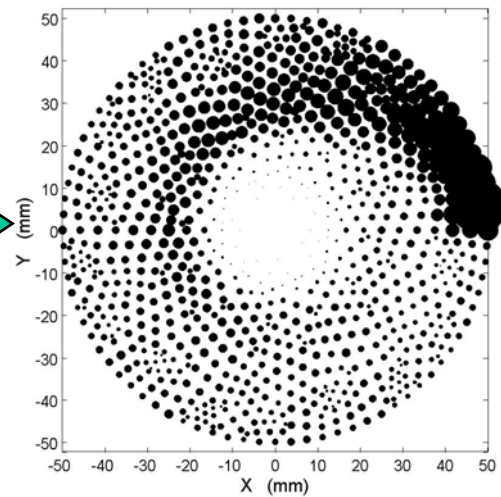
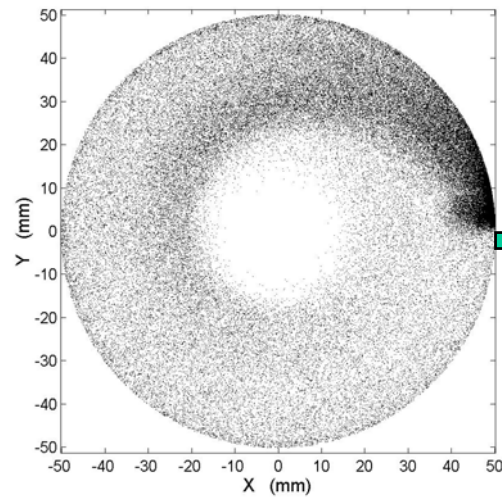
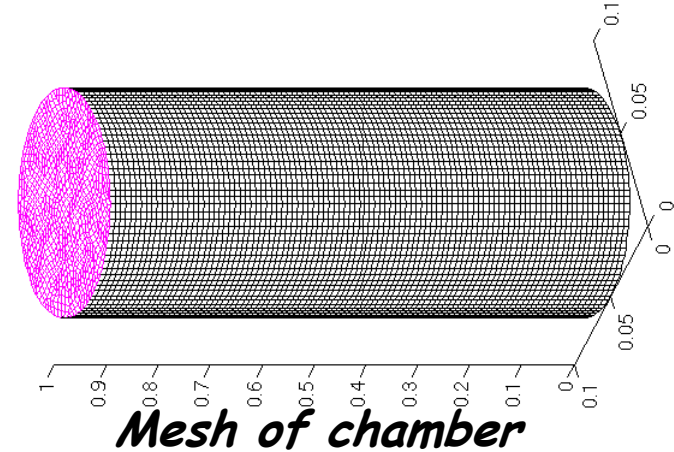
20 node element

Charge assignment

$$Q_i = N_i Q_0 \quad \sum_i N_i = 1$$

Real charge distribution

Meshed Charge distribution

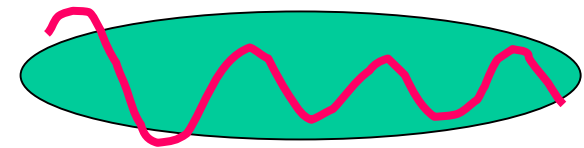


Classification of electron multipacting



If an electron can oscillate many times under the bam force during the passage of one bunch, then the bunch is called long bunch

$$\frac{\hat{z}\bar{\omega}}{\pi\beta c} \gg 1$$



Long bunch (Single bunch multipacting): PSR, SNS, JPAC, ISIS, ESS...

Short bunch (Multibunch multipacting): B-factories, PF, NLC damping ring, SPS, LHC, RHIC,.....

Source of electrons



Primary electrons

- Photon-electrons
(electron machine & LHC)
- Beam loss at the chamber surface (PSR, SNS, ISIS, ESS, JPARC)
- Residual gas ionization
- Stripped & scattered electrons

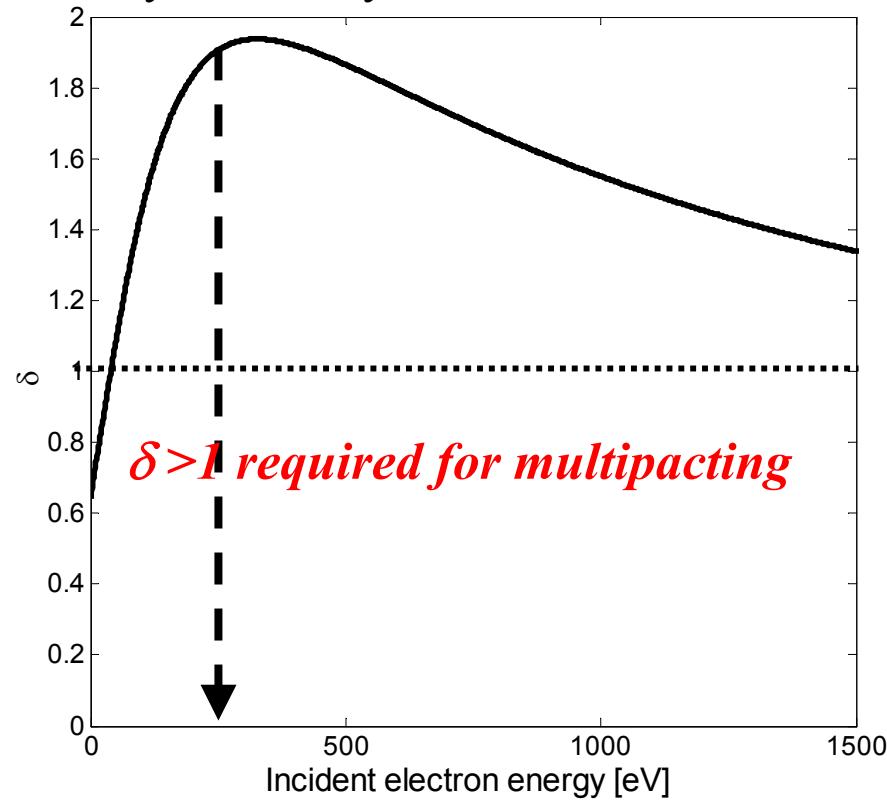
Table 1 Parameters for the SNS

| Parameter | Description | SNS |
|-----------------|-------------------------------|-----------------------|
| E (GeV) | Beam energy | 1.9 |
| C (m) | Circumference | 248 |
| N_p | Bunch population | 2.05×10^{14} |
| a_x, a_y (mm) | Transverse beam size | 28, 28 |
| τ_b (ns) | Bunch length | 700 |
| b (cm) | Beam pipe radius | 10 |
| P_l | Proton loss rate/turn | 1.1×10^{-6} |
| Y | Assumed proton-electron yield | 100 |

Secondary electrons



Secondary emission yield



courtesy P. He, M. Blaskiewicz

Key parameters for Multipacting (Strong **energy** and **SEY** dependence)

- SEY depend on the material property of the chamber surface (peak SEY and energy at peak SEY)
- Beam-electron interaction dependence (beam pattern, bunch current, bunch shape, bunch length, chamber size...)

SNS beam transverse profile shape

- **Square shape** resulting from correlated painting during the injection.
- Inclusion of the space charge causes rapid diffusion in azimuthal direction and results in **round beam shape**
- **Electron Multipacting (energy at the wall surface) does not depend on transverse profile**

Space charge field of uniform cylinder beam

$$E_r(r,t) = \begin{cases} \frac{\lambda(t)}{4\pi\epsilon_0} \frac{2}{r} & (r > a) \\ \frac{\lambda(t)}{4\pi\epsilon_0} \frac{2r}{a^2} & (r < a) \end{cases}$$
$$U(r,t) = \begin{cases} \frac{\lambda(t)}{4\pi\epsilon_0} \left(1 + 2 \ln \frac{r}{a}\right) & (r > a) \\ \frac{\lambda(t)}{4\pi\epsilon_0} \frac{r^2}{a^2} & (r < a) \end{cases}$$

Nonlinear Hamiltonian of the radial motion

$$H = \frac{p^2}{2m} + eU(r,t)$$

The longitudinal beam force is neglected

Nonlinear Oscillation Frequency

$$T = 4.0 \int_0^{r_{amp}} \frac{dr}{v(r)} = 4.0 \int_0^{r_{amp}} \frac{dr}{\sqrt{2\Phi e / m}}$$

$$T = \begin{cases} 4.0 \sqrt{\frac{\pi \epsilon_0 m}{\lambda e}} \left(\sqrt{2} a \arcsin \frac{1}{\sqrt{1 + 2 \ln(r_{amp}/a)}} + \int_a^{r_{amp}} \frac{dr}{\sqrt{\ln(r_{amp}/r)}} \right) \\ 2\pi a \sqrt{\frac{2\pi \epsilon_0 m}{\lambda e}} & (r_{amp} \leq a) \end{cases}$$

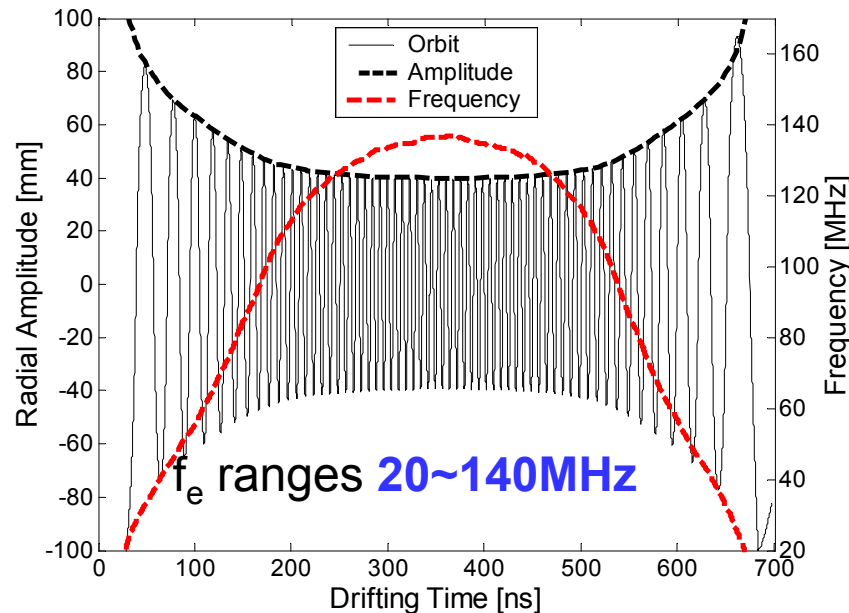
Adiabatic invariant

$$\frac{1}{\omega_e^2} \frac{d\omega_e}{dt} \ll 1 \text{ (if } t > 20\text{ns and } t < 680\text{ns for SNS)}$$

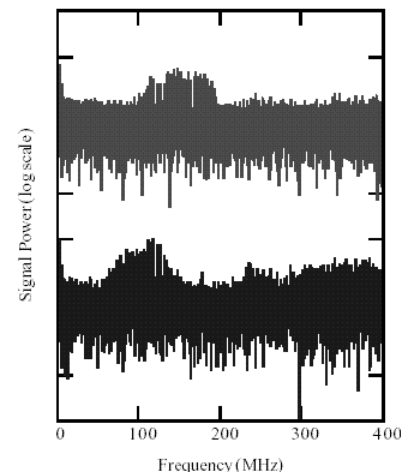
$$J = \oint pdq$$

$$J = \begin{cases} \frac{\pi r_{amp}^2}{a} \sqrt{\frac{me\lambda}{2\pi\epsilon_0}} & (r_{amp} < a) \\ 4a \sqrt{\frac{me\lambda}{2\pi\epsilon_0}} \left(\frac{\sqrt{2}}{2} x^{1/2} + \frac{1+2x}{2} \operatorname{arctg} \frac{1}{\sqrt{2x}} + \frac{\sqrt{2}}{a} \int_a^{r_{amp}} \sqrt{\ln \frac{r_{amp}}{r}} dr \right) & (r_{amp} > a) \end{cases}$$

$x = \ln(r_{amp}/a)$



Oscillation amplitude and frequency



LANL PSR
beam spectrum

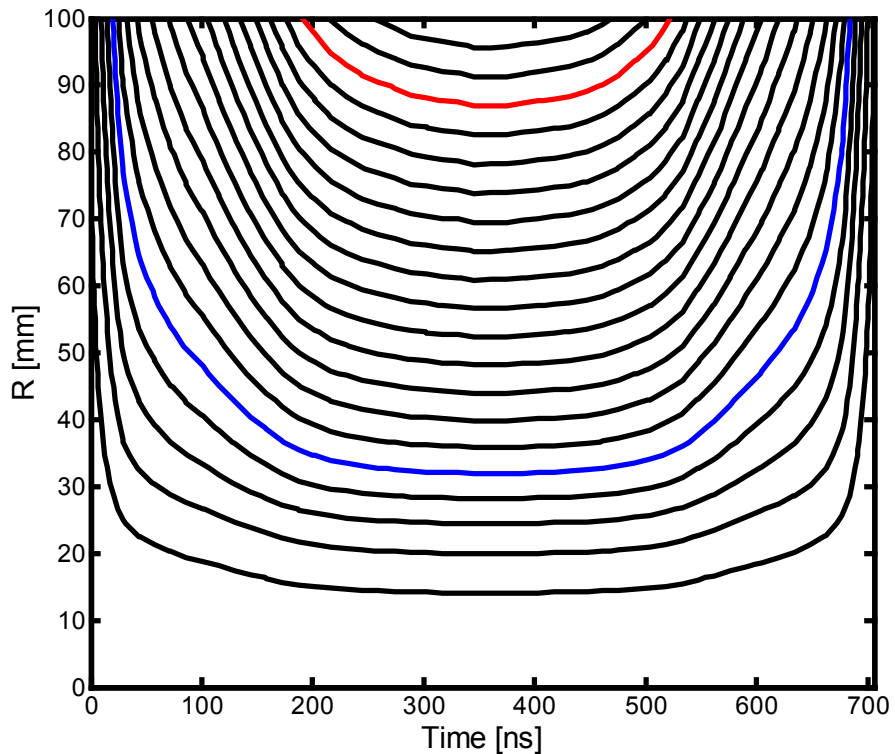
50~150MHz

courtesy
Robert J. Macek

Oscillation amplitude from adiabatic invariant



- Contour plot from adiabatic invariant can clearly describe the electron orbit
- All electron emitted (including gas ionization) before the bunch center or survived from last bunch gap can be trapped (inside beam for the survived electrons) during the bunch passage and are released at the bunch tail. The trapped electrons, most of them are the survived electrons from the last bunch gap, contribute to beam dynamics (instabilities)
- All electrons which emitted from the wall after bunch center will directly drift to the opposite of wall surface. The straight drifting electrons contribute to multipacting due to their short drifting time & high energy when they hit the wall surface.

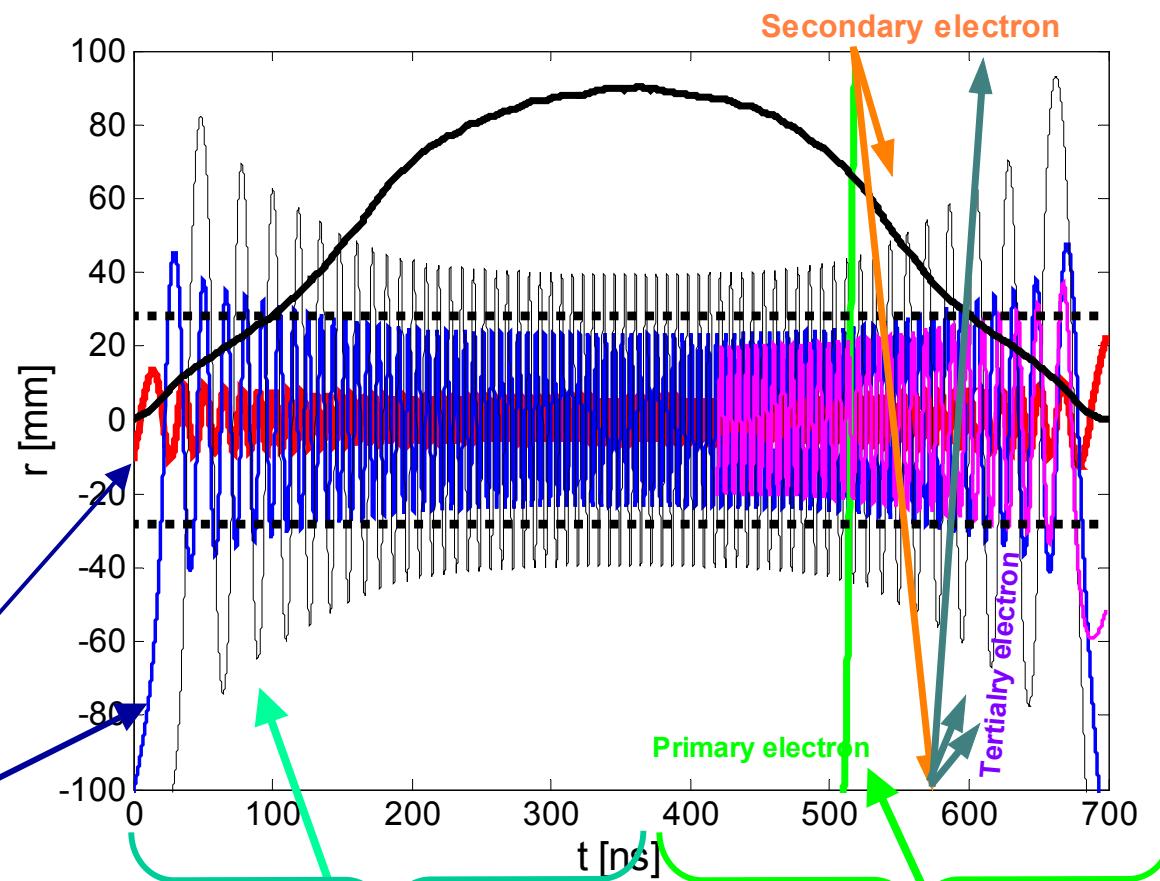


Contour plot of the oscillation amplitude resulting from adiabatic invariant for SNS beam

Particle motion vs. instability & multipacting



Typical orbits of various electrons trapped by SNS beam, bold solid line shows the longitudinal beam profile shape and the dashed back lines show the beam size



Electrons survived from the bunch gap (beam instabilities)

Electrons emitted before bunch center (trapped and lost after bunch center)

Electrons emitted after the bunch center (multipacting)

Electrons by ionization
(beam instabilities)

Energy Gain of straight drifting electron & Mechanism of trailing edge multipacting



Assuming the beam line density is a linear function of time during the short electron drifting time($\sim 10\text{ns}$)

$$\Delta E = -\frac{1}{2} \sqrt{\frac{me}{2\pi\varepsilon_0}} \beta c \left(a(2\zeta - 1) \arcsin \frac{1}{\sqrt{\zeta}} + a \sqrt{2 \ln \frac{b}{a}} + \sqrt{2}\zeta \int_a^b \frac{dr}{\sqrt{\ln(b/r)}} - \frac{1}{\sqrt{2}} \int_a^b \frac{1+2\ln(r/a)}{\sqrt{\ln(b/r)}} dr \right) \frac{\partial \lambda}{\partial z} \frac{1}{\sqrt{\lambda}}$$

$$\zeta = 1 + 2 \ln(b/a)$$

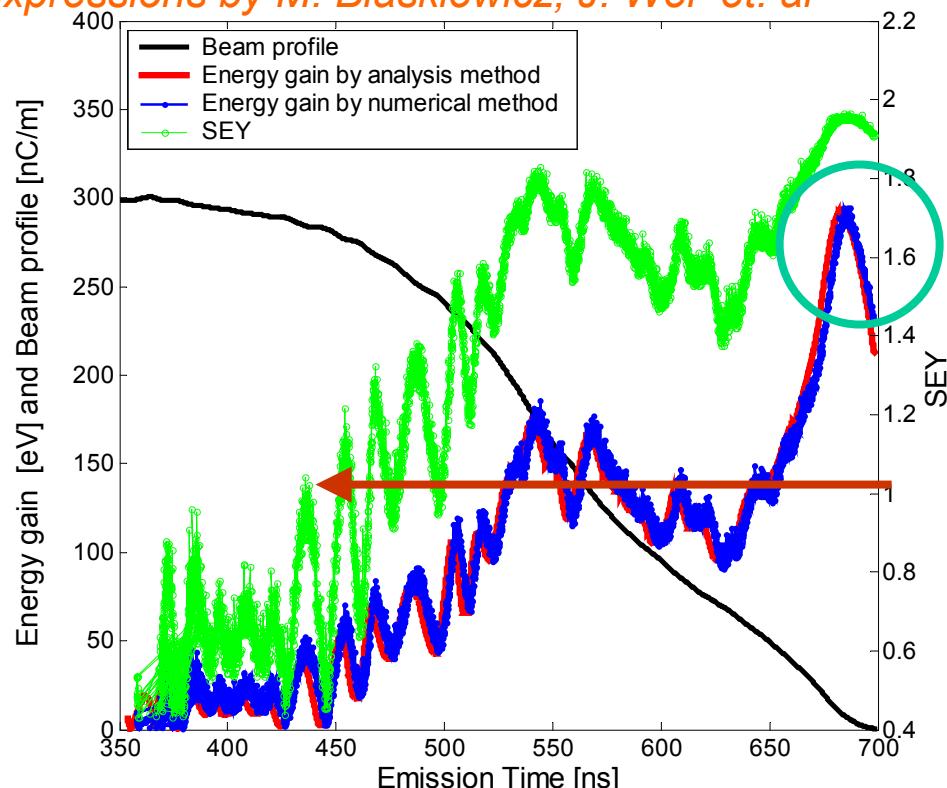
Also see other expressions by M. Blaskiewicz, J. Wei et. al

a : beam size, b , chamber radius, λ is beam line density

Longitudinal beam profile factor

$$\text{Factor}_{\text{profile}} = -\frac{\partial \lambda}{\partial z} \frac{1}{\sqrt{\lambda}}$$

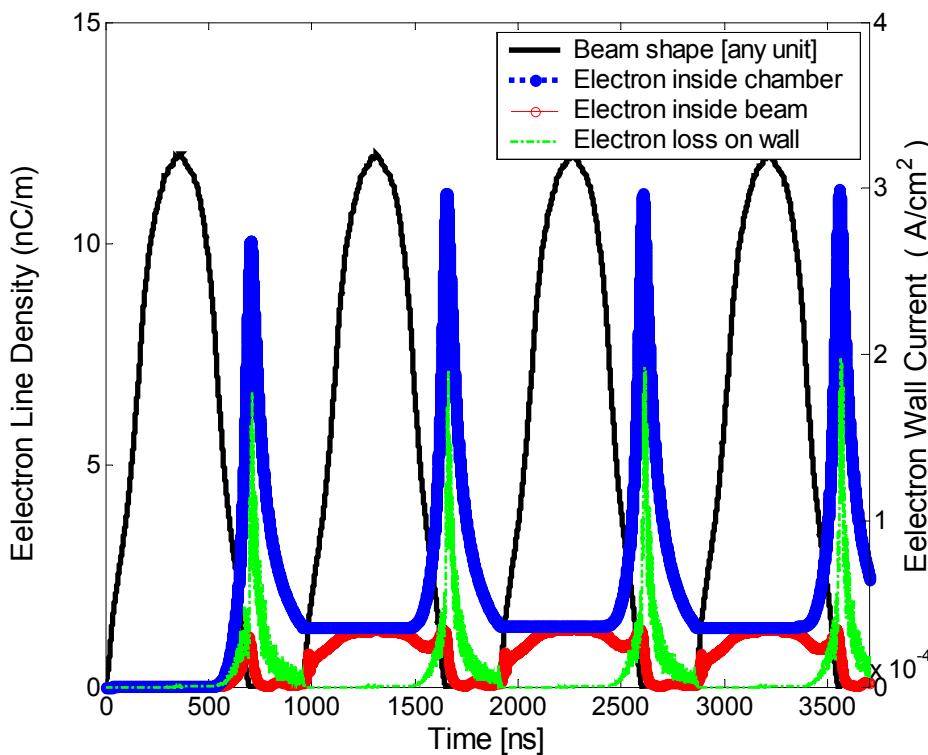
- Good agreement with numerical method
- Calculated SEY can be used to predict the multipacting directly
- Adiabatic motion and Energy gain can explain the mechanism of "trailing edge multipactor"



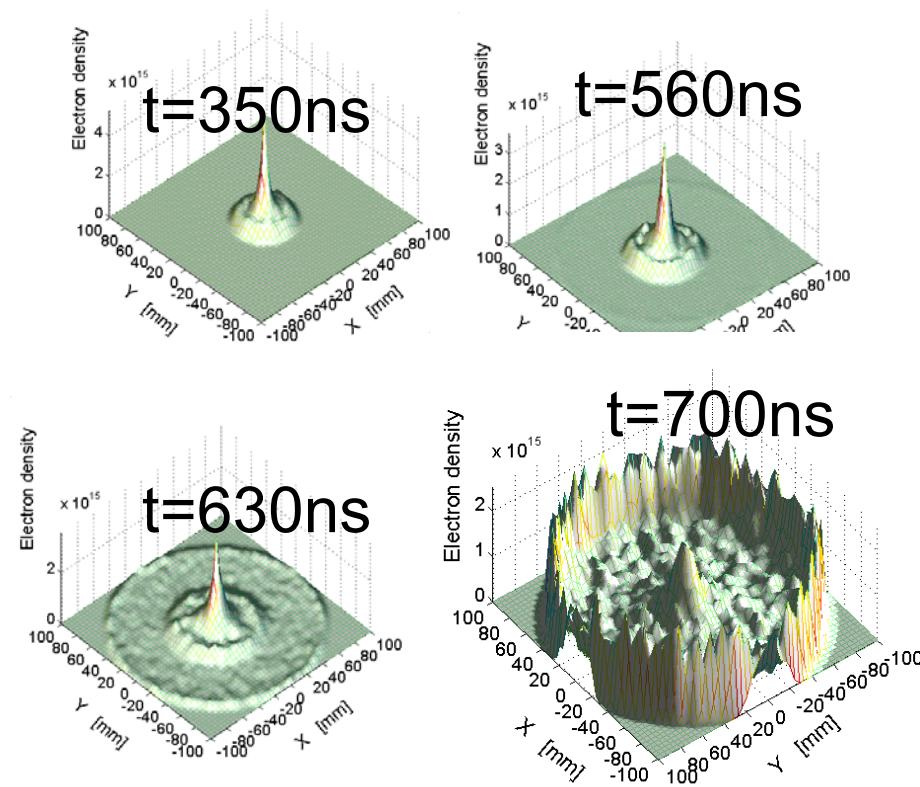
E-cloud in drift region



- Single bunch multipacting
- Trailing Edge Multipacting
- All surviving electron from the last gap are trapped inside beam during the bunch passage (Contributing to beam instabilities)
- Bunch gap is important for *beam dynamics*

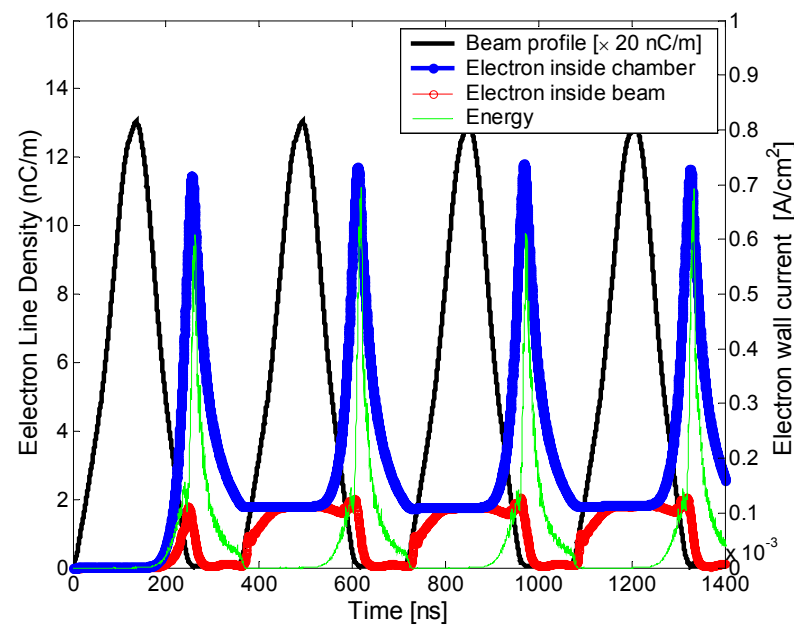
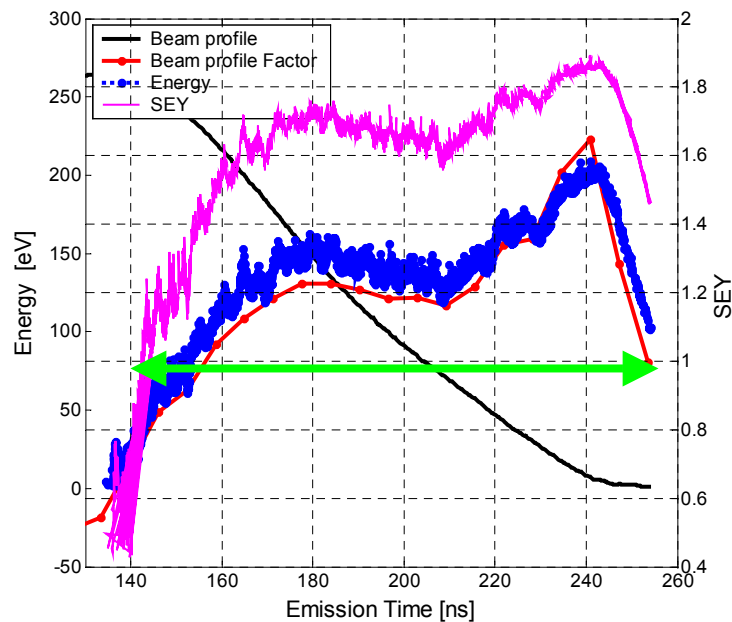


E-cloud build-up in SNS drift region

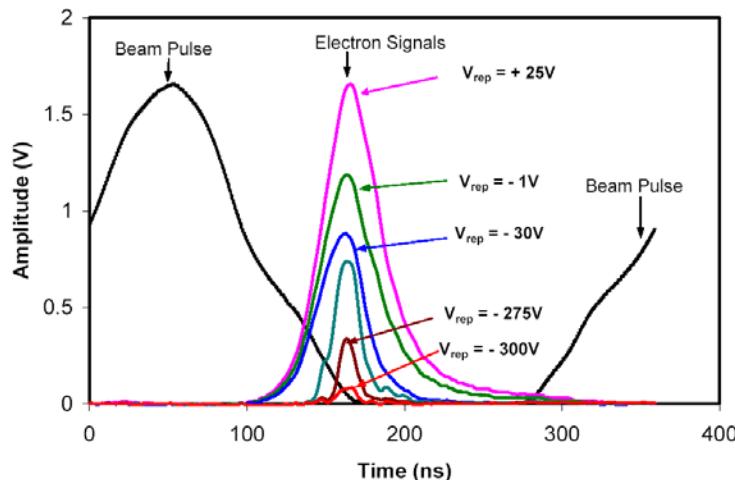


E-cloud distribution in different time

Eccloud in PSR



Electron signals from RFA in straight section 4



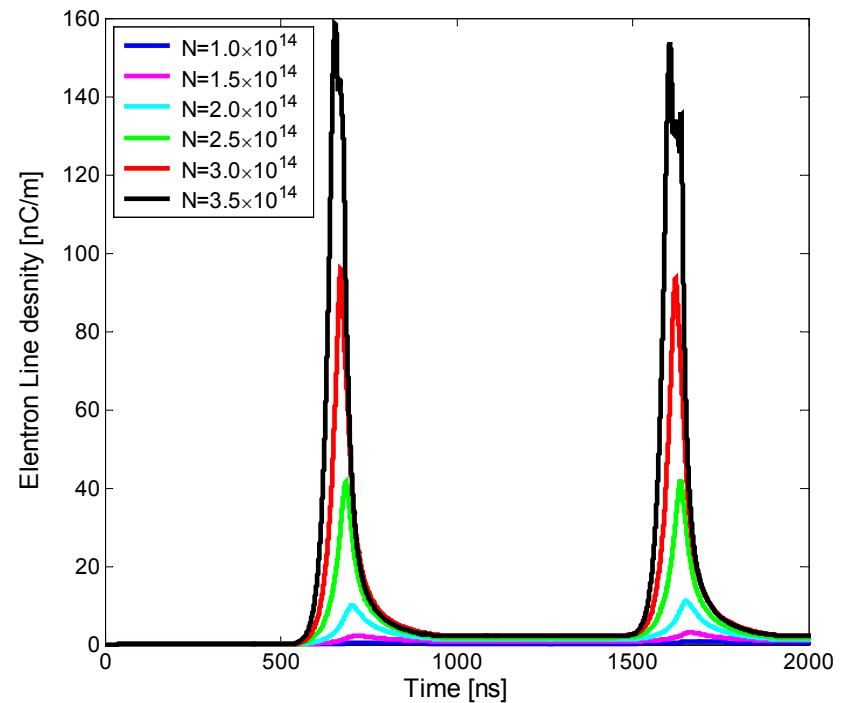
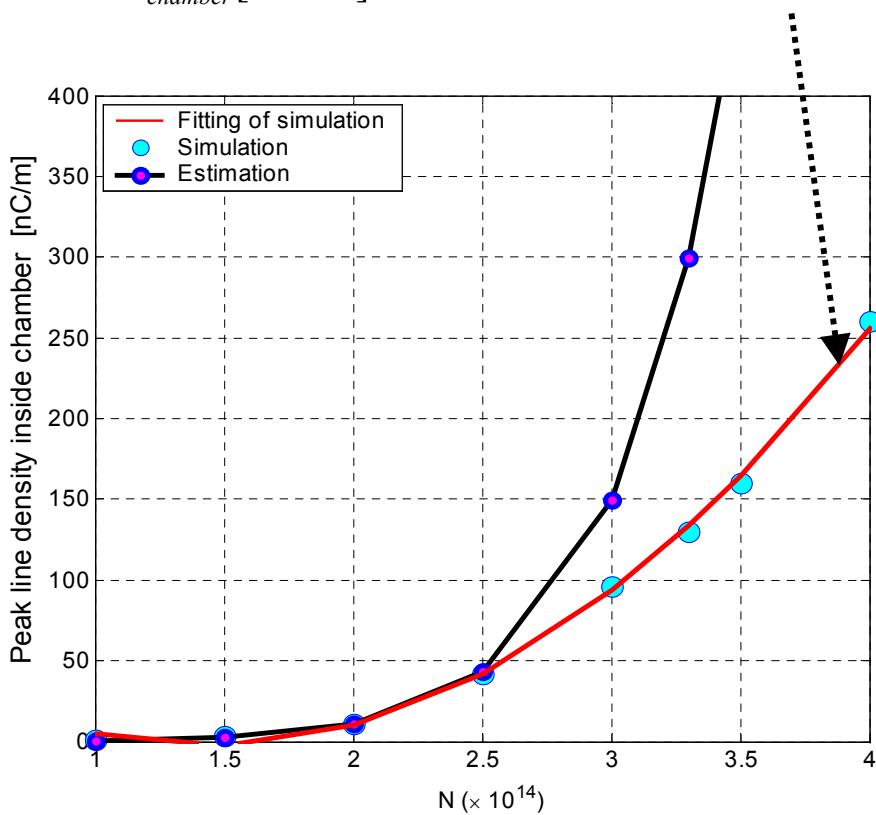
courtesy Robert J. Macek

Beam intensity effects (I)



- High beam intensity causes high electron energy gain
- High beam intensity increases multipacting frequency $f_{multipacting} \propto \sqrt{\lambda}$
- Space charge slows the growth of electron density inside chamber when strong multipacting case happens

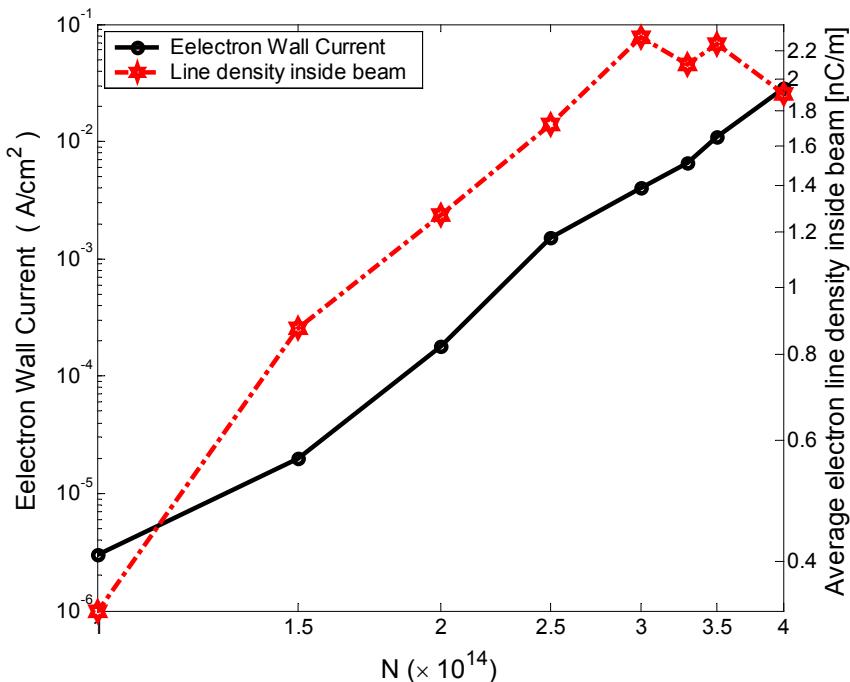
$$\lambda_{chamber} [nC/m] = 78 - 112 \times 1.0^{-14} N + 39 \times 1.0^{-28} N^2$$



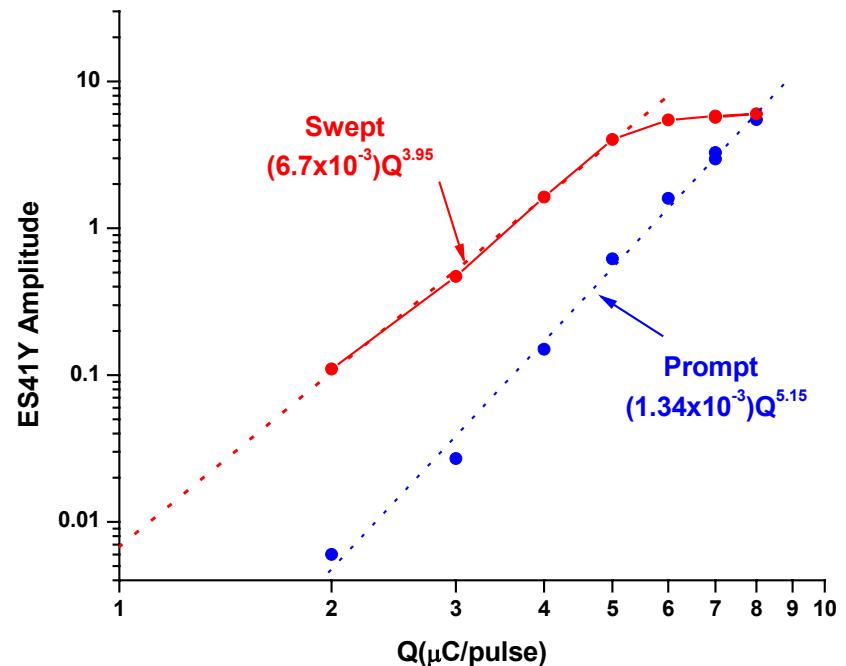
Beam intensity effects (II)



- Space charge makes the electron density inside beam saturated when strong multipacting case happens



SNS, simulation



LANL PSR, Experiment, R. Macek

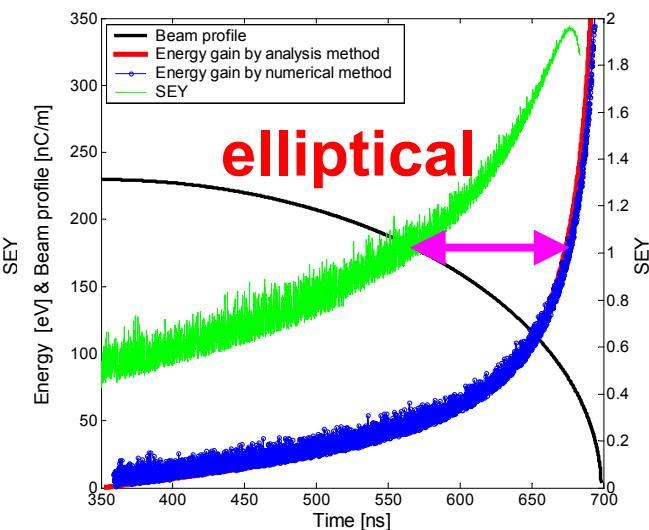
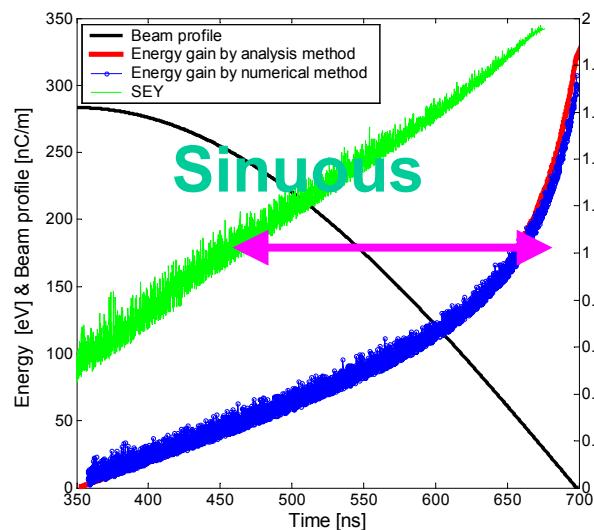
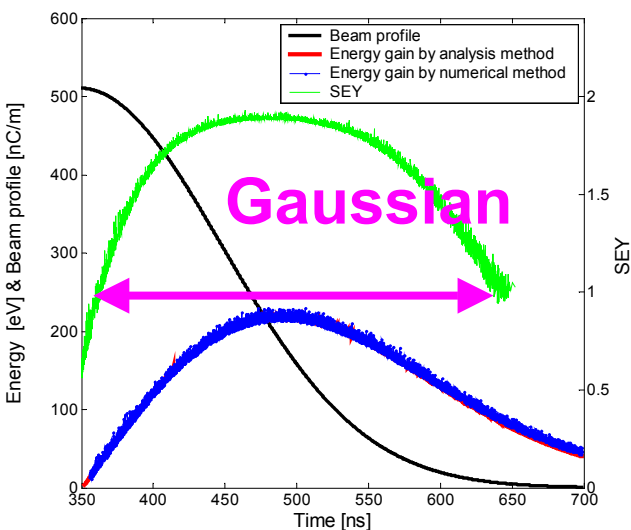
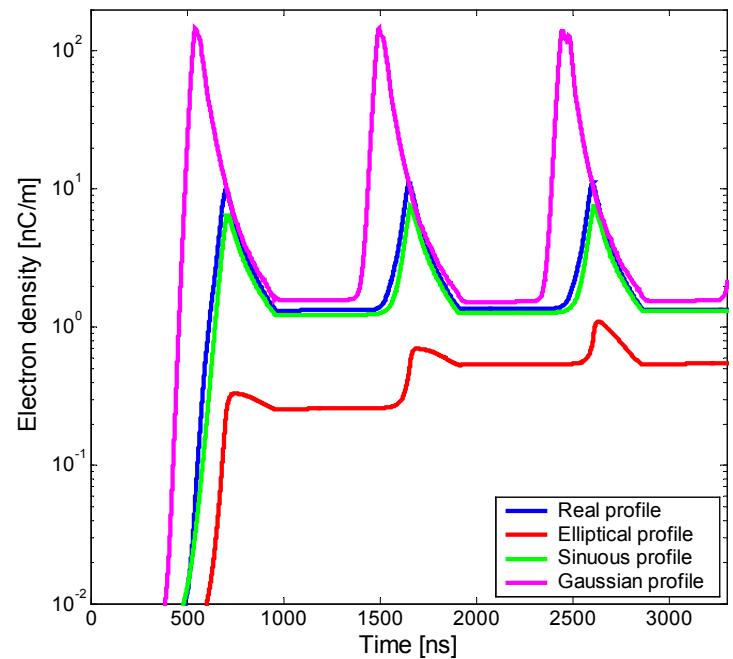
Important Factors Related to Electron multipacting(1)



Longitudinal Beam Profile

For assumed Gaussian, sinuous & elliptical beam profile:

- Gaussian profile excites the strongest multipacting due to long bunch tail
- Elliptical profile has the weakest multipacting
- Electron cloud of the real profile is close to that of the sinuous profile



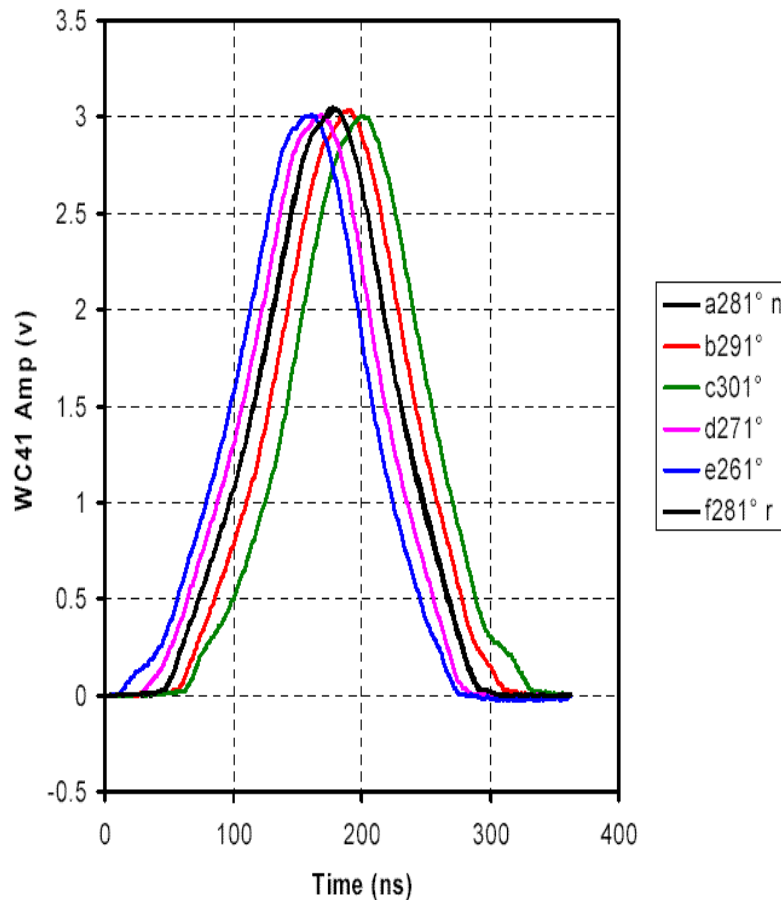
Longitudinal beam profile effects (cont.)



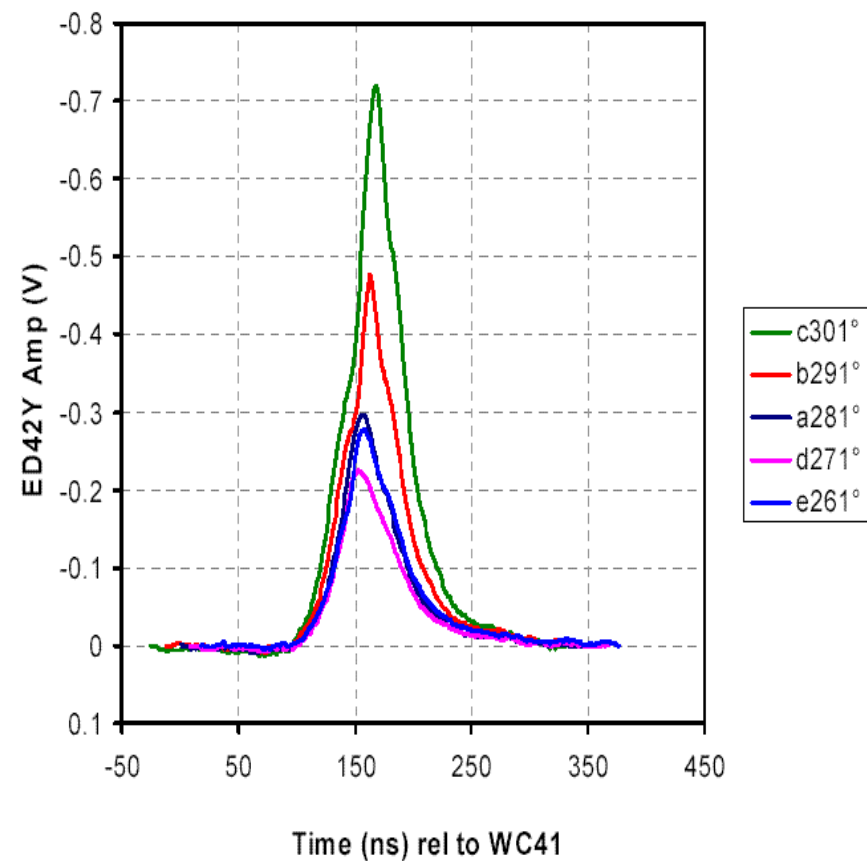
Electron signals vs. bunch shape

(LANL PSR experiment, courtesy Robert J. Macek, ecloud'02)

Effect of rf Buncher phase variations



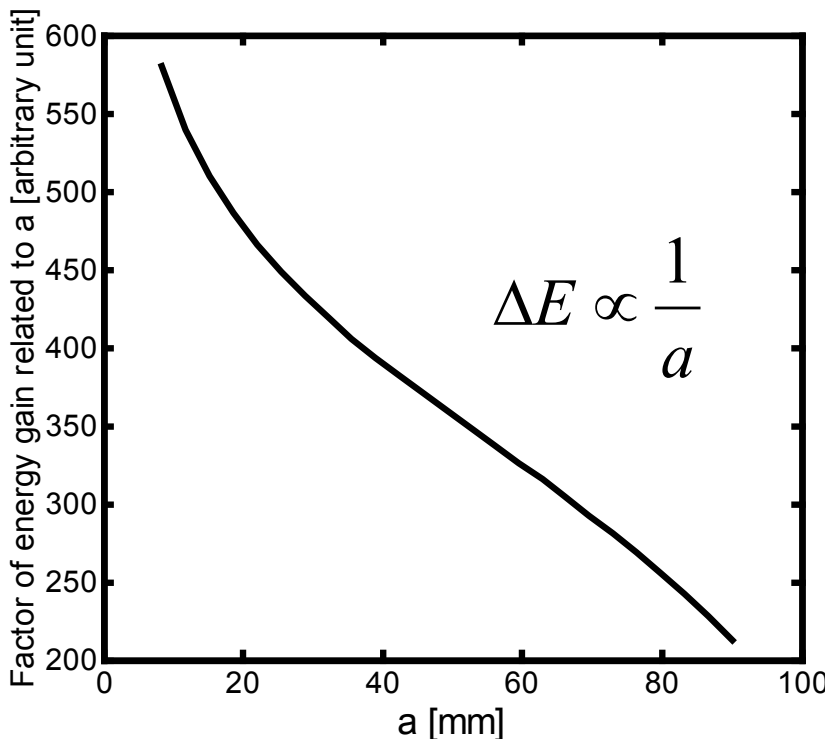
ED42Y signals for rf phase changes



Transverse Beam Size Effects

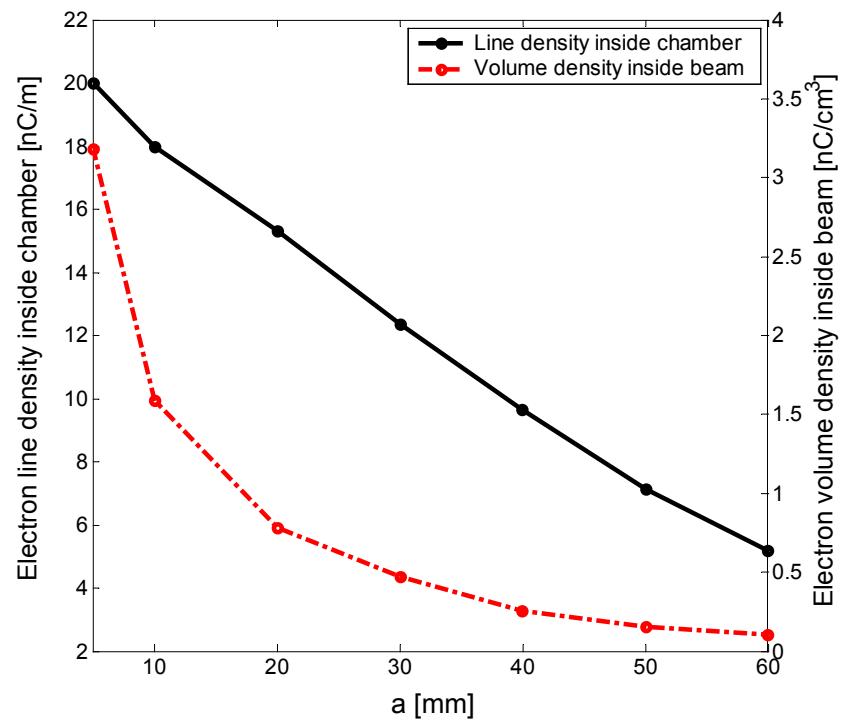


- A smaller beam size contributes to stronger space charge field and hence larger electron energy gain and stronger multipacting.
- Instabilities is sensitive to a . Small a , strong instability



$$\lambda_{chamber}[nC/m] = 21 - 0.27a[\text{mm}]$$

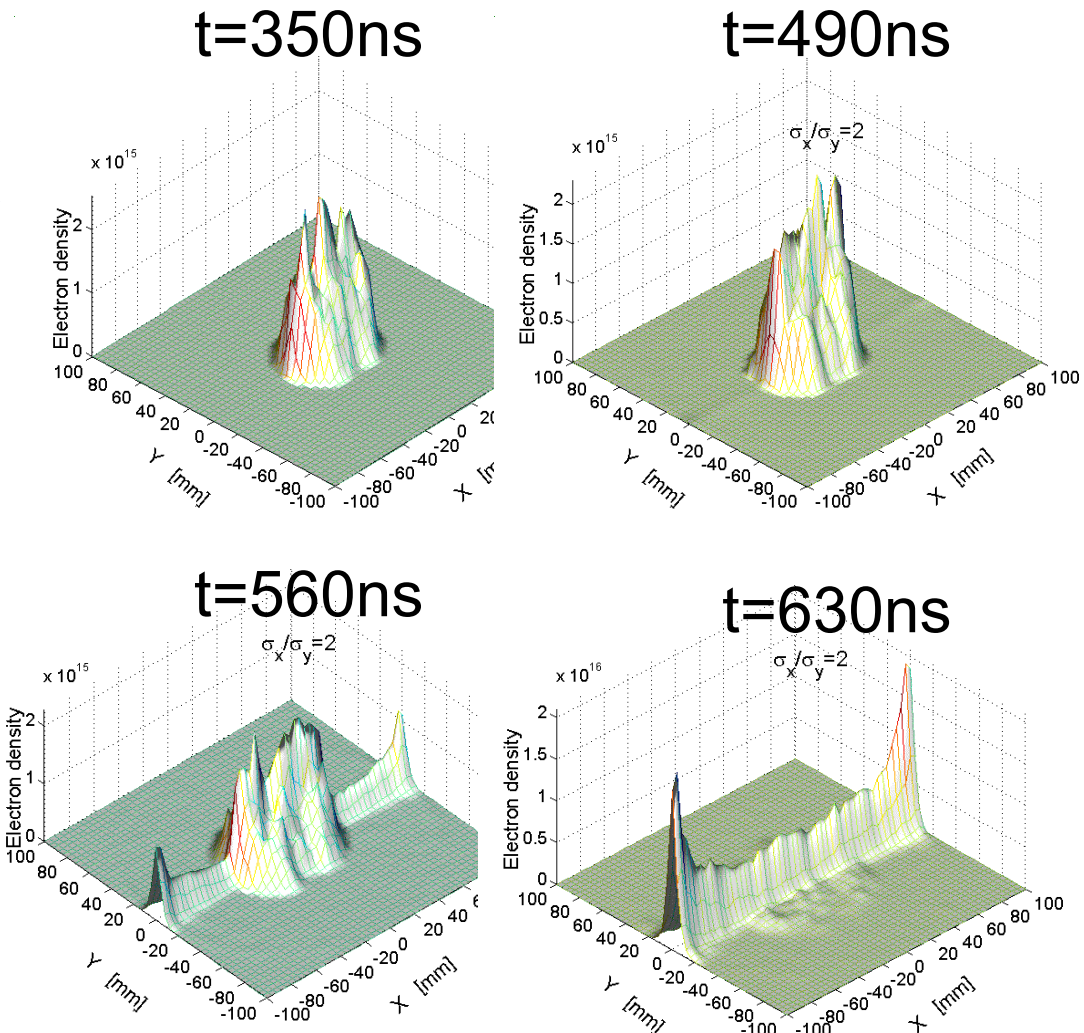
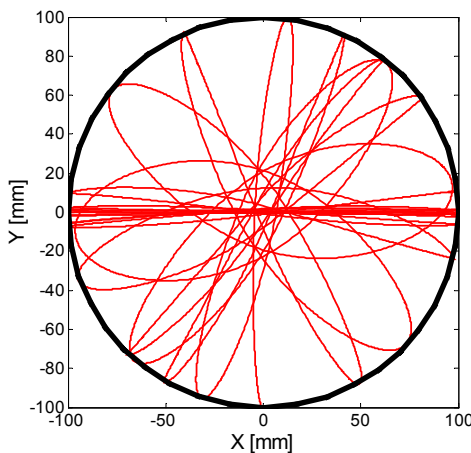
$$\rho_{cen}[nC/cm^3] = 4.9e^{-0.1a[\text{mm}]}$$



Flat beam effect on EC distribution



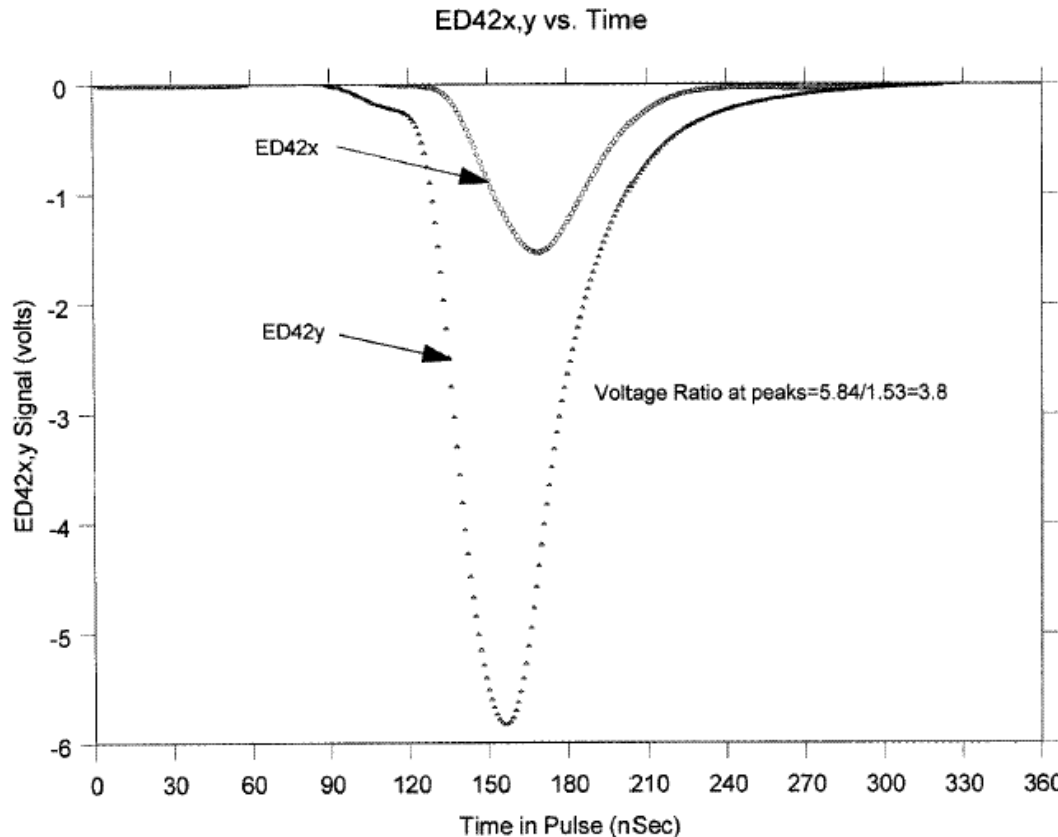
- Flat beam $\sigma_x : \sigma_y = 2:1$
- Stronger multipacting in larger beam size direction due to the “polarization effect” of strong beam space charge force



PSR experimental study----flat beam



- Qualitatively agrees with LANL PSR observation
- Instability & detector

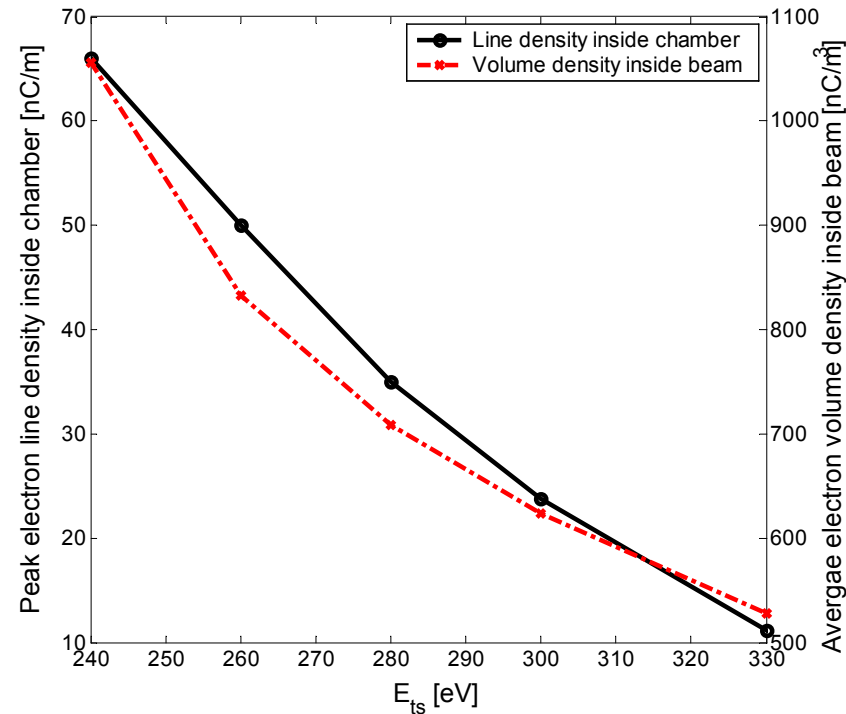
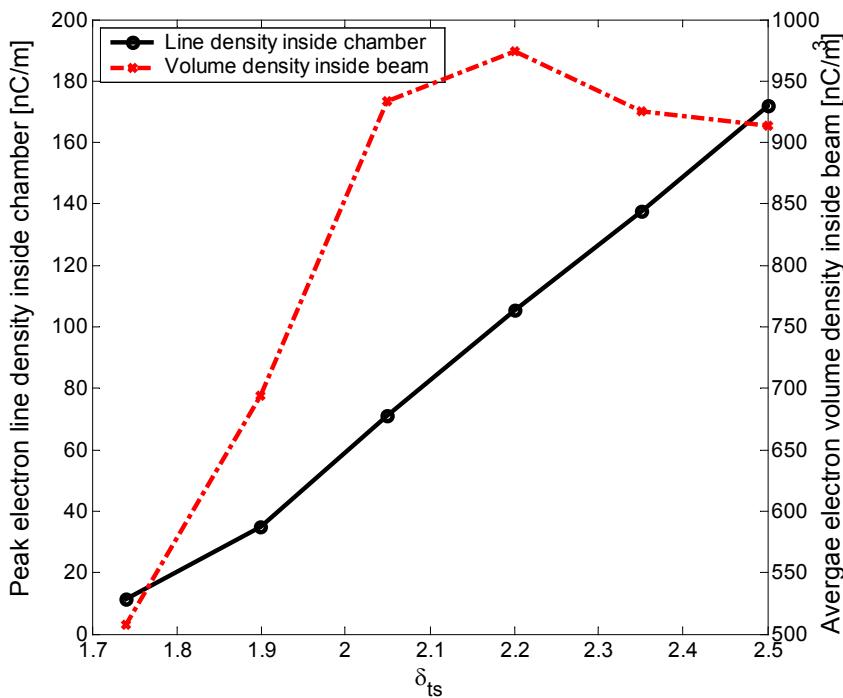


A. Browman Two-stream-2000

Peak SEY and Energy at Peak SEY



- E-cloud density inside chamber is a linear function of peak SEY and energy at peak SEY.
- E-cloud density inside chamber (and hence Instability growth rate) increases linear with peak SEY and finally saturates at some level.
- E-cloud density inside chamber (and hence Instability growth rate) decreases with the energy at peak SEY.



Electron motion in dipole magnets



- Dipole magnetic field $\mathbf{B}=(0, B_y, 0)$
- Beam electric field $\mathbf{E}=(E_x, E_y, 0)$

$$\frac{dv_y}{dt} = eE_y / m$$

$$v_x = v_{x0} \cos \omega t + v_{z0} \sin \omega t + \frac{E_{x0}}{B} \sin \omega t + \frac{1}{\omega B} \frac{dE_x}{dt} - \frac{1}{\omega B} \left(\frac{dE_x}{dt} \right)_0 \cos \omega t - \frac{1}{\omega B} \cos \omega t \int_0^t \frac{d^2 E_x}{dt^2} \cos \omega t dt - \frac{1}{\omega B} \sin \omega t \int_0^t \frac{d^2 E_x}{dt^2} \sin \omega t dt$$

$$v_z = v_{z0} \cos \omega t - v_{x0} \sin \omega t + \frac{E_{x0}}{B} \cos \omega t - \frac{E_x}{B} - \frac{1}{B} \cos \omega t \int_0^t \frac{dE_x}{dt} \cos \omega t dt + \frac{1}{B} \sin \omega t \int_0^t \frac{dE_x}{dt} \sin \omega t dt$$

- In strong dipole magnet ($B \sim 1T$ for SNS) $\left| \frac{1}{\omega E_x} \frac{dE_x}{dt} \right| \ll 1$
- Electron motion \approx **gyration motion** + **translation** (cross-field drifting) + movement along B-field lines
- The kinetic energy of gyration motion and cross-field drifting is **smaller** comparing with the kinetic energy in B-field direction.

Electron energy gain in strong dipole magnet

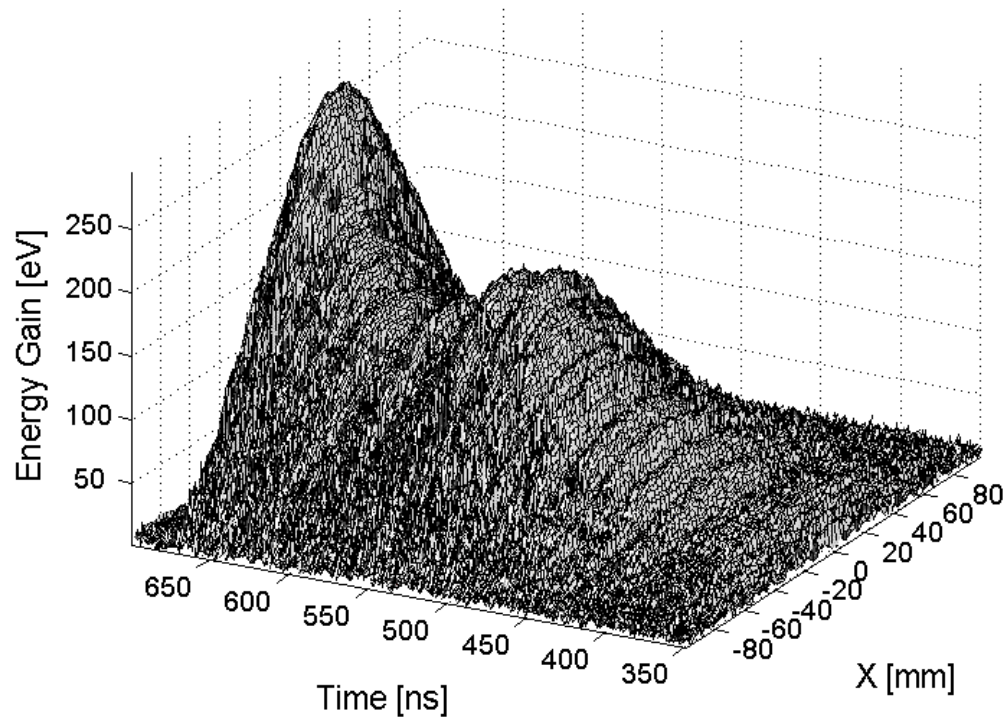
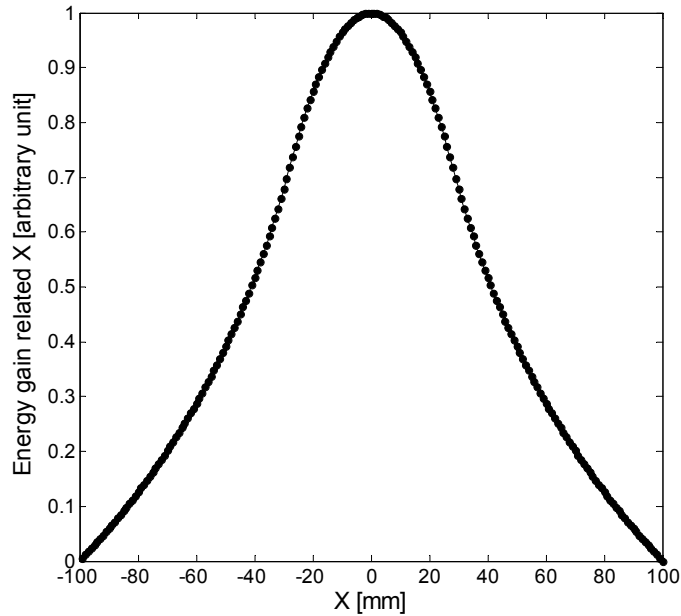


$$\begin{aligned} \Delta E(X) = & -c\beta \sqrt{\frac{me}{2\pi\varepsilon_0}} \frac{\partial\lambda}{\partial z} \frac{1}{\sqrt{\lambda}} \left(1 - \frac{X^2}{a^2} + \ln \frac{b^2}{a^2} \right) \left(aG + \int_{\sqrt{a^2-X^2}}^{\sqrt{b^2-X^2}} \left(\ln \frac{b^2}{X^2+y^2} \right)^{-1/2} dy \right) \\ & + \frac{1}{2} c\beta \sqrt{\frac{me}{2\pi\varepsilon_0}} \frac{\partial\lambda}{\partial z} \frac{1}{\sqrt{\lambda}} \int_0^{\sqrt{a^2-X^2}} \frac{y^2}{a^2} \left[\ln \left(1 - \frac{X^2}{a^2} + \ln \frac{b^2}{a^2} + \frac{y^2}{a^2} \right) \right]^{-1/2} dy \\ & + \frac{1}{2} c\beta \sqrt{\frac{me}{2\pi\varepsilon_0}} \frac{\partial\lambda}{\partial z} \frac{1}{\sqrt{\lambda}} \int_{\sqrt{a^2-X^2}}^{\sqrt{b^2-X^2}} \left(1 - \frac{X^2}{a^2} + \ln \frac{X^2+y^2}{a^2} \right) \left[\ln \left(\frac{b^2}{X^2+y^2} \right) \right]^{-1/2} dy \quad (|X| < a) \end{aligned}$$

$$\Delta E(X) = -c\beta \sqrt{\frac{me}{2\pi\varepsilon_0}} \frac{\partial\lambda}{\partial z} \frac{1}{\sqrt{\lambda}} \left[\frac{b^2}{X^2} \int_0^{\sqrt{b^2-X^2}} \left(\ln \frac{b^2}{X^2+y^2} \right)^{-1/2} dy - \frac{1}{2} \int_0^{\sqrt{b^2-X^2}} \frac{X^2+y^2}{X^2} \left(\ln \frac{b^2}{X^2+y^2} \right)^{-1/2} dy \right]$$

$$G = \arcsin \left[\frac{\sqrt{a^2 - X^2}}{a} \left(1 - \frac{X^2}{a^2} + \ln \frac{b^2}{X^2+a^2} \right)^{-1/2} \right] \quad (|X| > a)$$

Electron energy gain in strong dipole magnet

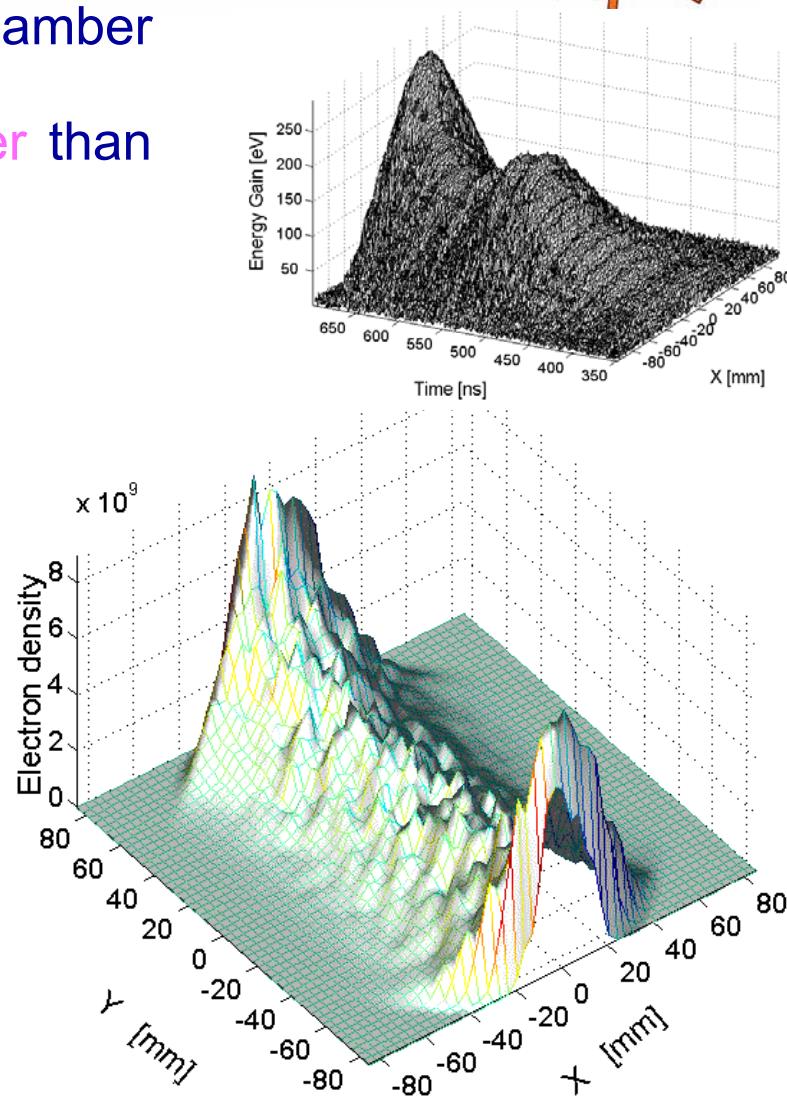
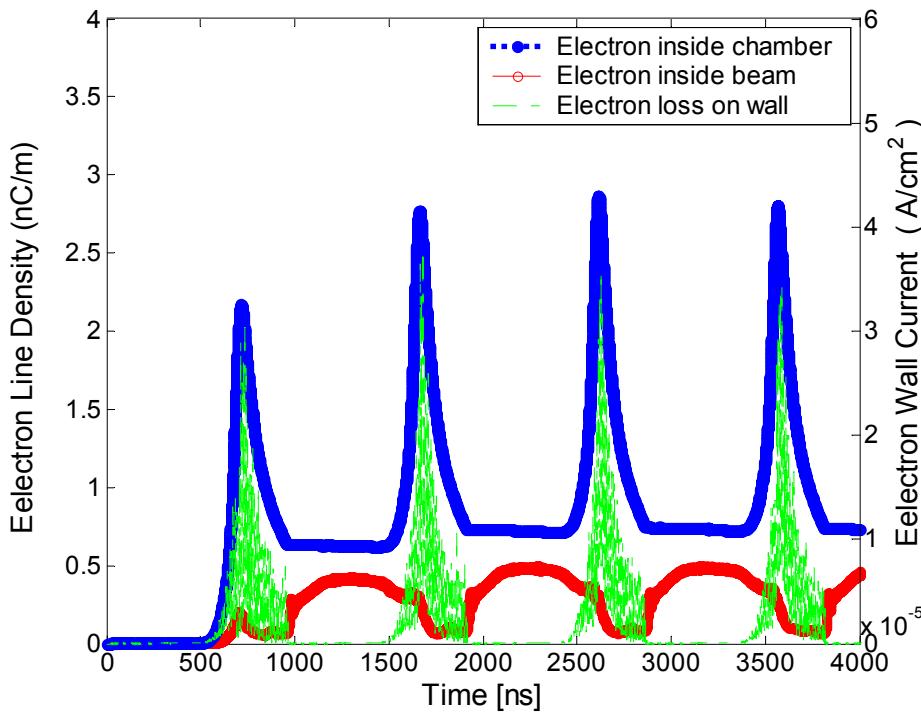


Energy gain at the wall surface for different X-coordinates. Left plot shows the electron energy gain as a function of horizontal coordinate. It is normalized by the peak energy gain at the chamber center $X=0$. Right plot shows the energy gain of direct drifting electrons in SNS dipole magnets with $B_y=7935$ Gauss.

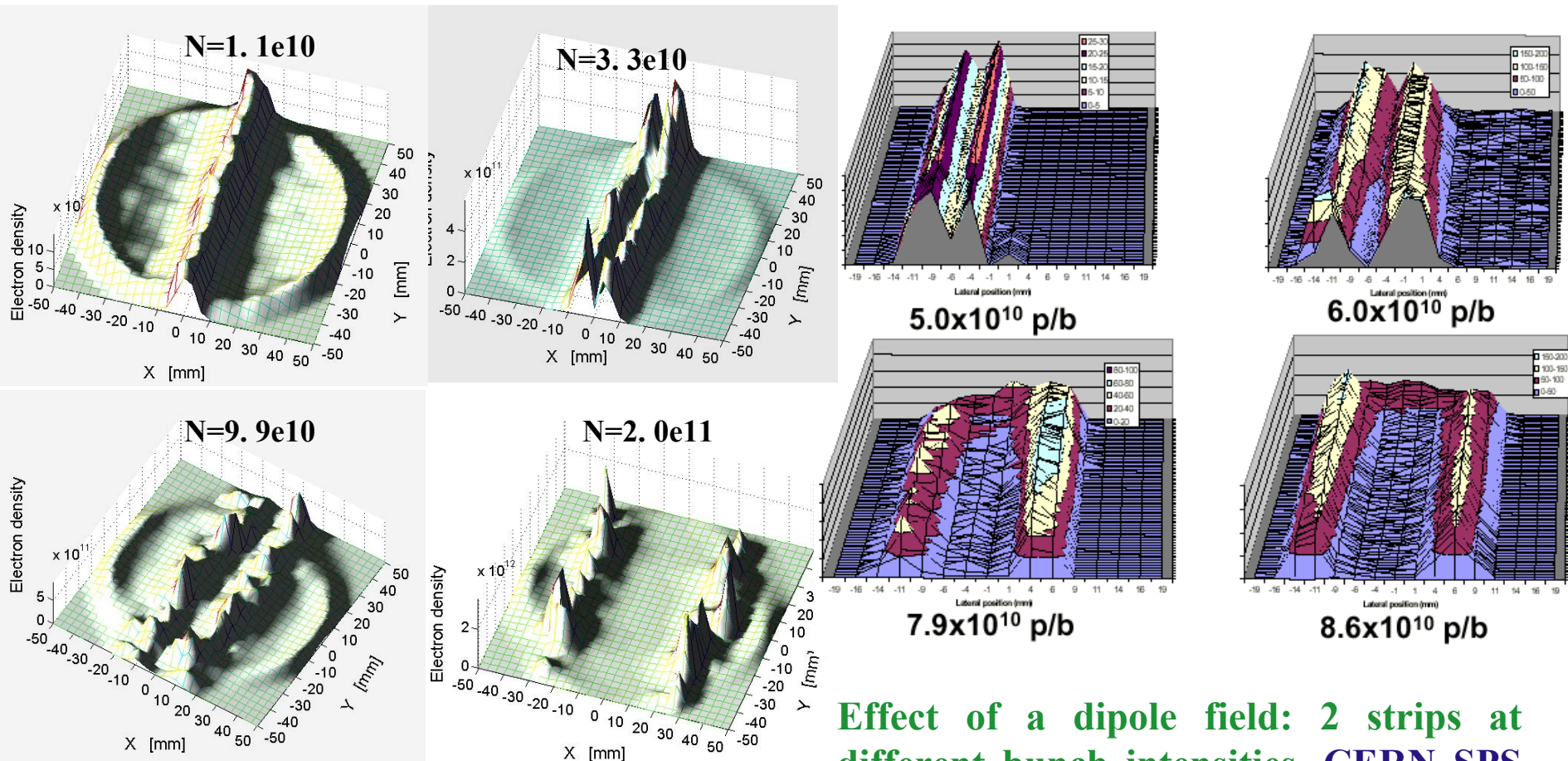
Multipacting in Dipole magnets (By=0.79T)



- Multipacting happen at the horizontal chamber center (**1 strip**, agree with estimation)
- E-cloud density is about 2 times smaller than the drift region



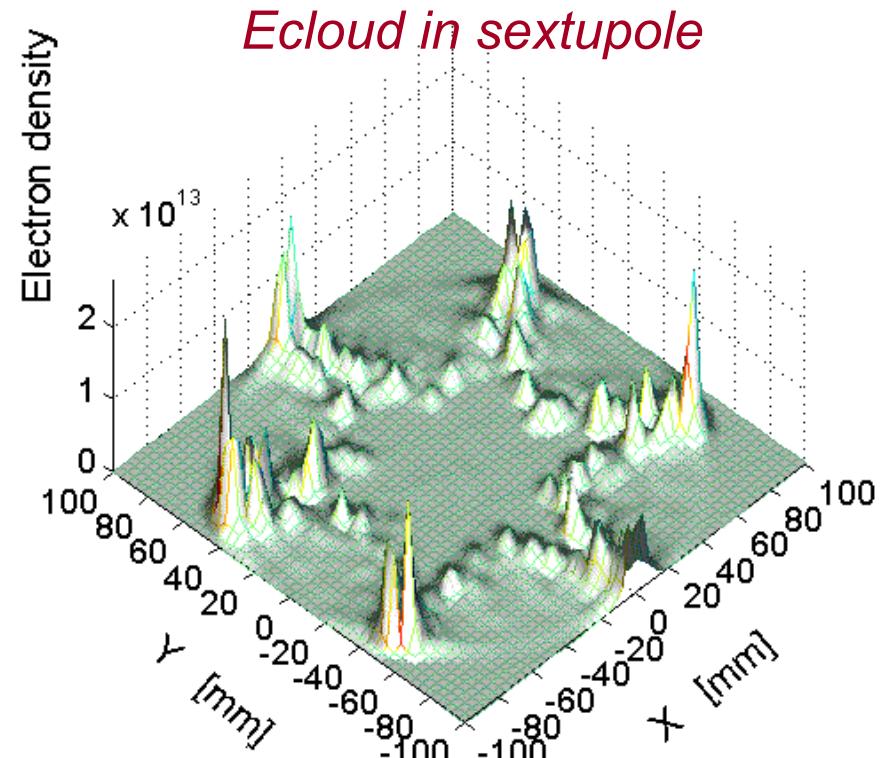
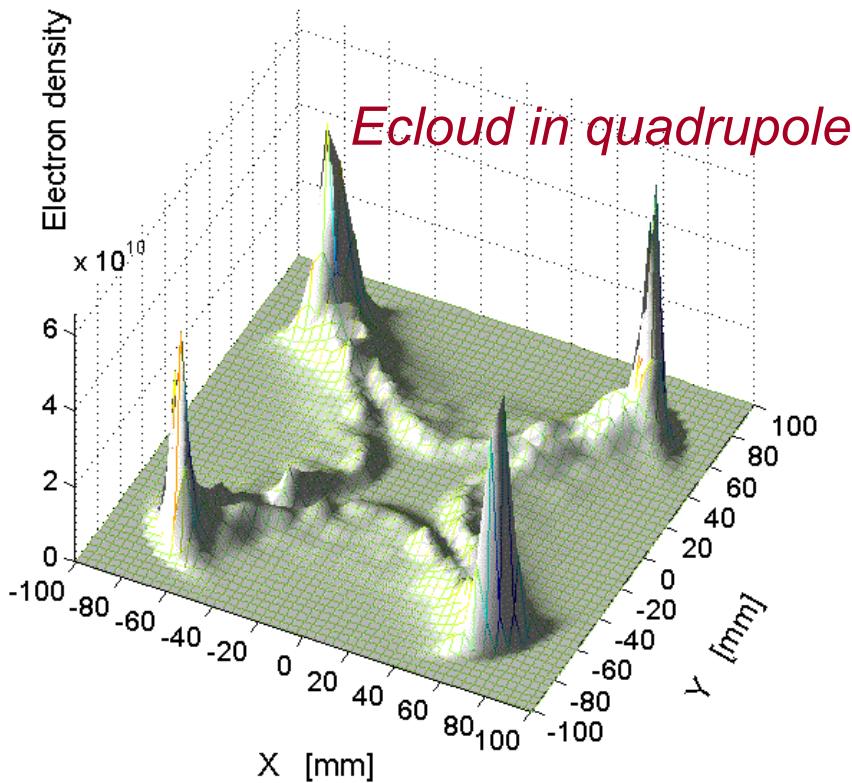
Bunch current effects on Multipacting in dipole for short bunch---strip position and lost charge density



KEKB LER, simulation

Effect of a dipole field: 2 strips at different bunch intensities, CERN SPS experimental results, J. M.Jimenez, ECloud'02, CERN, 2002

E-cloud in Quadrupole and Sextupole magnets



- Weak multipacting happens only near the middle of the pole surface
- No Trapping for long bunch! (trap was suspected in PSR, PSR-94-005)

Invariance value of motion

$$W = \frac{mv^2}{2} = \frac{mv_{\parallel}^2}{2} + \frac{mv_{\perp}^2}{2} = \text{constant}$$

$$\frac{1}{2}mv_{\parallel}^2 + \mu_m B = \text{const}$$

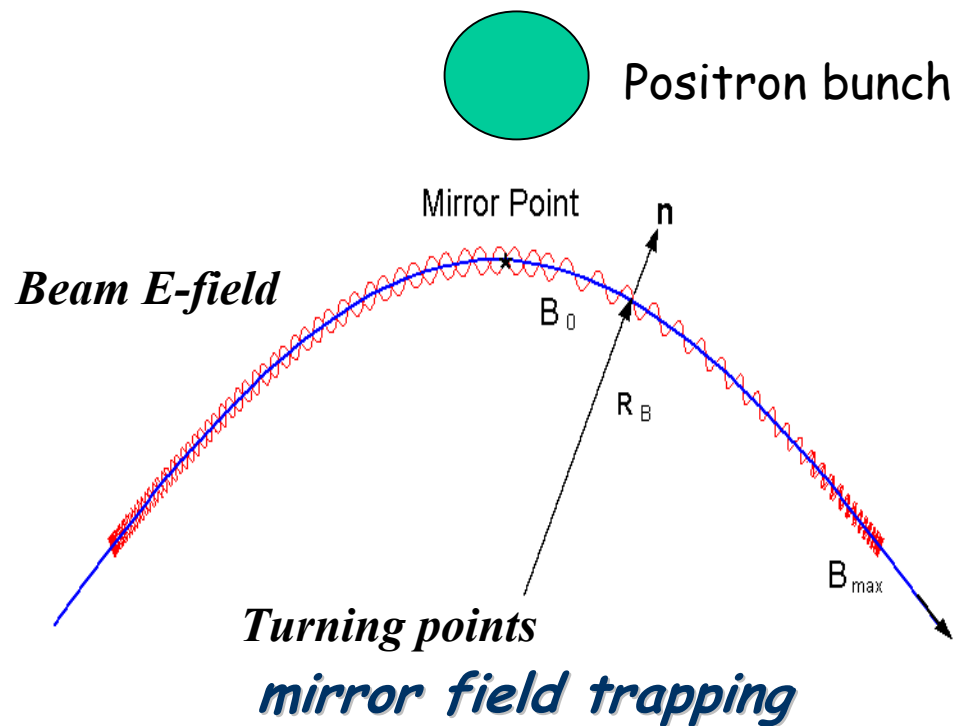
→ Reflective Points: $v_{\parallel} = 0$

Trapping condition

$$\Gamma_{trap} > 1$$

$$\Gamma_{trap} = \frac{F_v}{F_B} = \frac{v_{\perp 0}^2}{v_{\perp 0}^2 + v_{\parallel 0}^2} \frac{B_{max}}{B_0}$$

Trap factor is constant if no other force (except B force) disturbs the electron and smaller than 1.0, no trapping



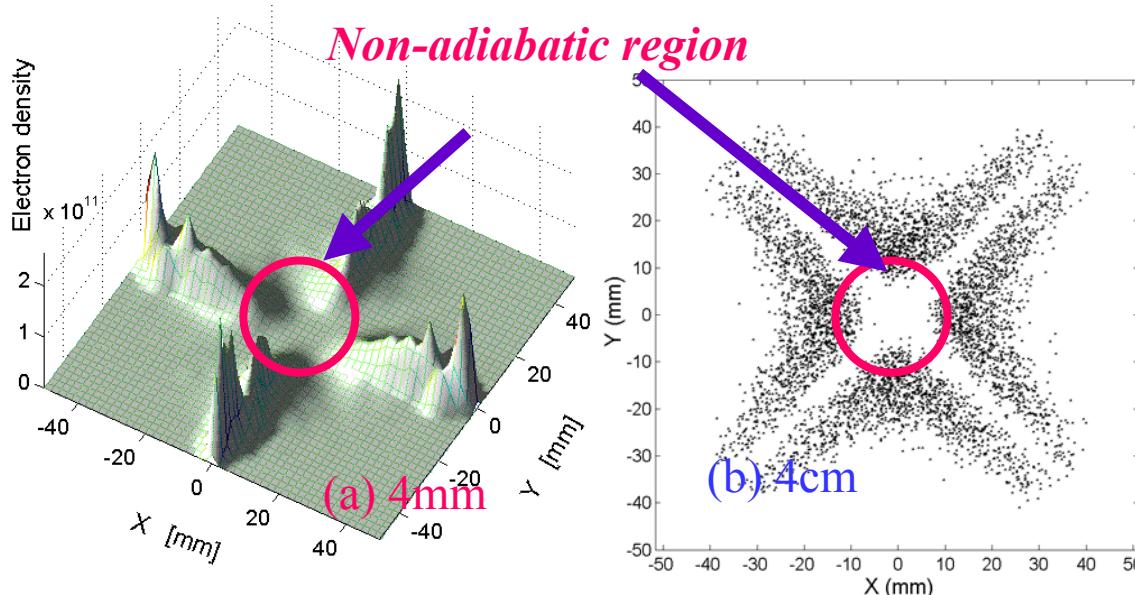
$$\Gamma_{trap} = \left. \frac{v_{\perp 0}^2}{v_{\perp 0}^2 + v_{\parallel 0}^2} \right|_{\text{at the emission point}} = \text{constant} \leq 1$$

Trap requirement for positron bunch

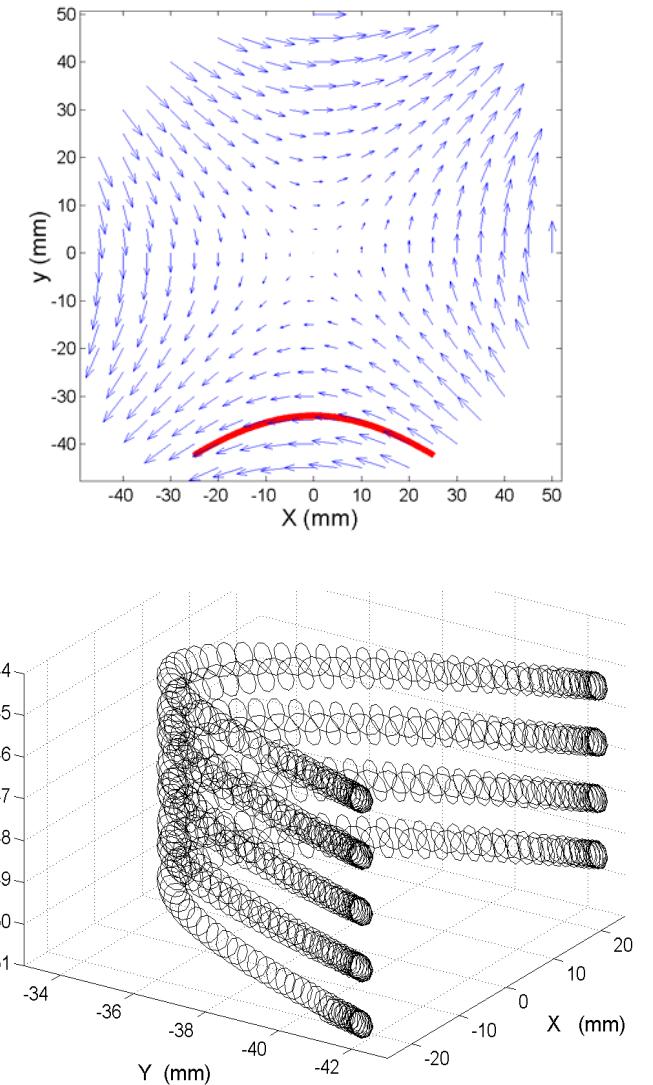
Bunch length should be shorter than period of gyration

motion

$$\sigma_l < \frac{2\pi cm}{e} \frac{1}{B} \rightarrow \sigma_l (mm) < 10.7 / B(T)$$



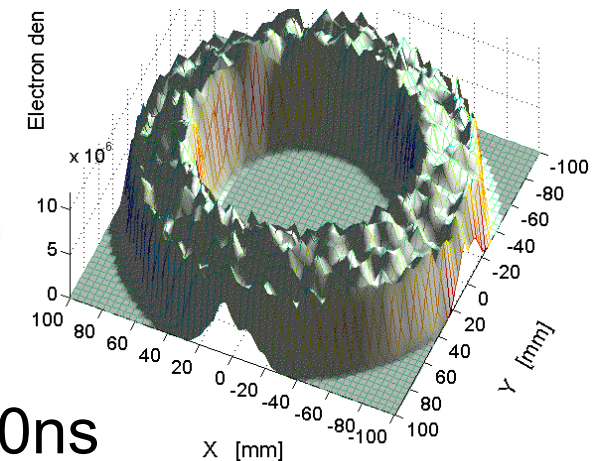
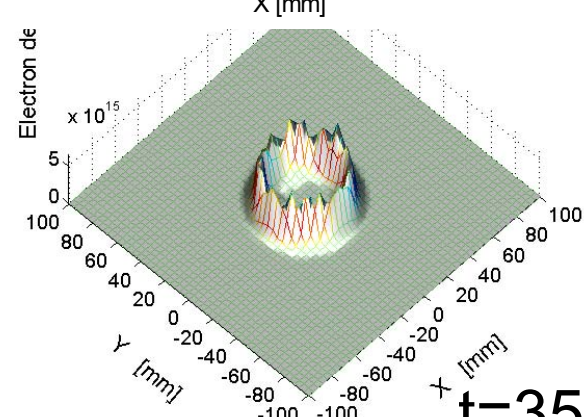
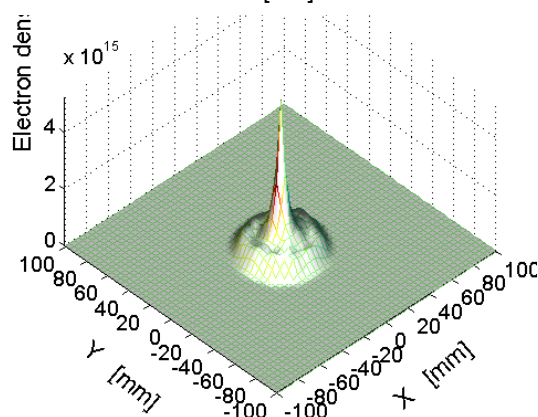
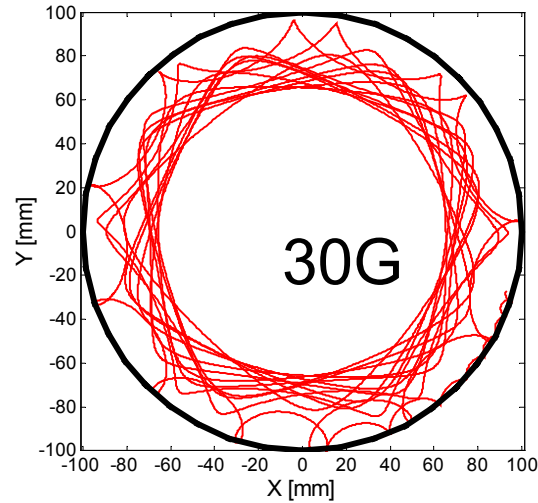
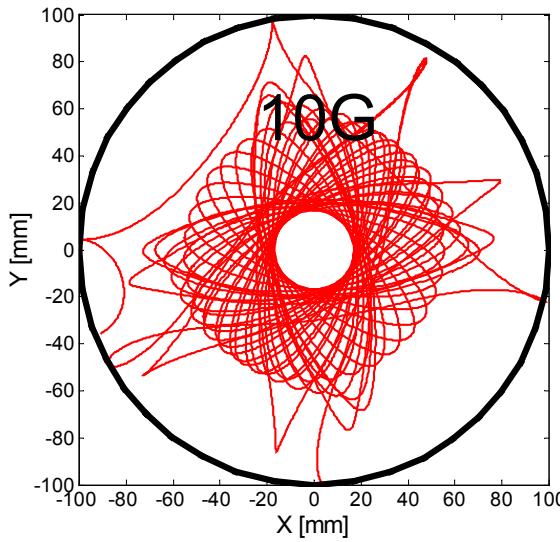
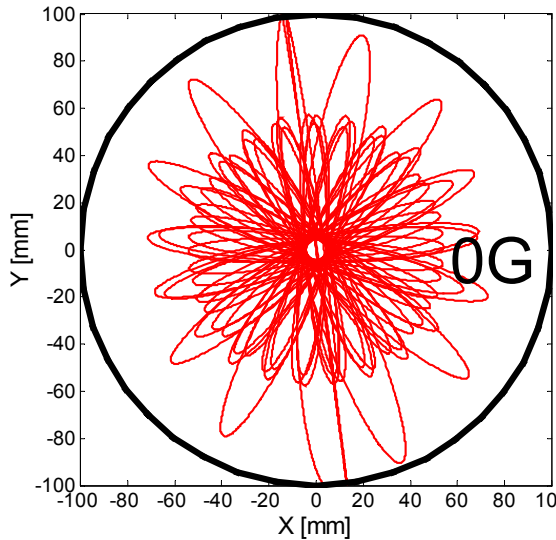
Trapped photoelectron distribution in quadrupole magnet with field gradient 10.3 T/m during the train gap for different bunch length



Uniform Solenoid effects

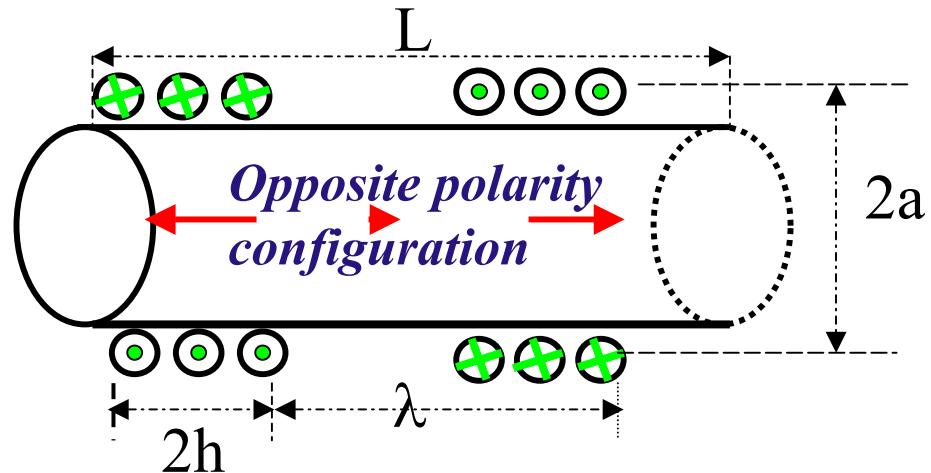
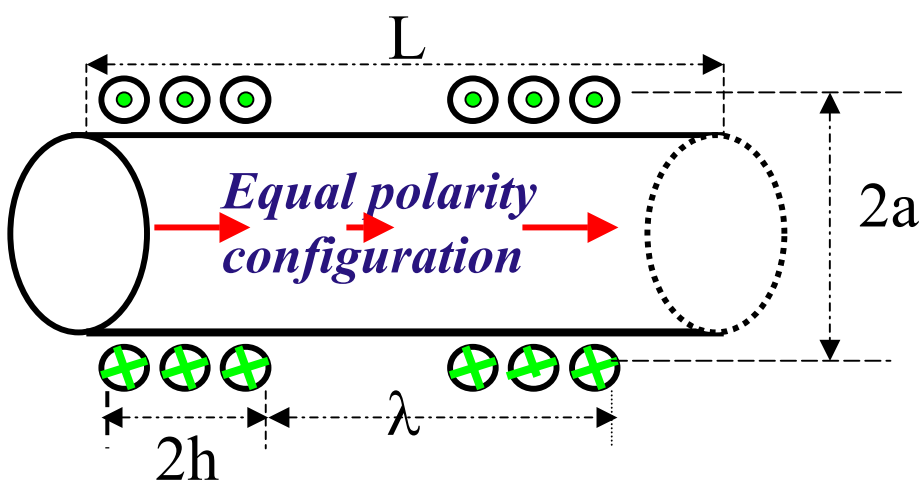


- 30G Solenoid field can reduce the e-cloud density with a factor **2000**!
- Zero density within beam



t=350ns

Solenoid---Configuration



$$B_r = B_0 \frac{2ka}{\pi} \sum_{n=1}^{\infty} \sin nhk K_1(nka) I_1(nkr) \sin nkz$$

$$B_z = B_0 \left(\frac{2h}{\lambda} + \frac{2ka}{\pi} \sum_{n=1}^{\infty} \sin nhk K_1(nka) I_0(nkr) \cos nkz \right)$$

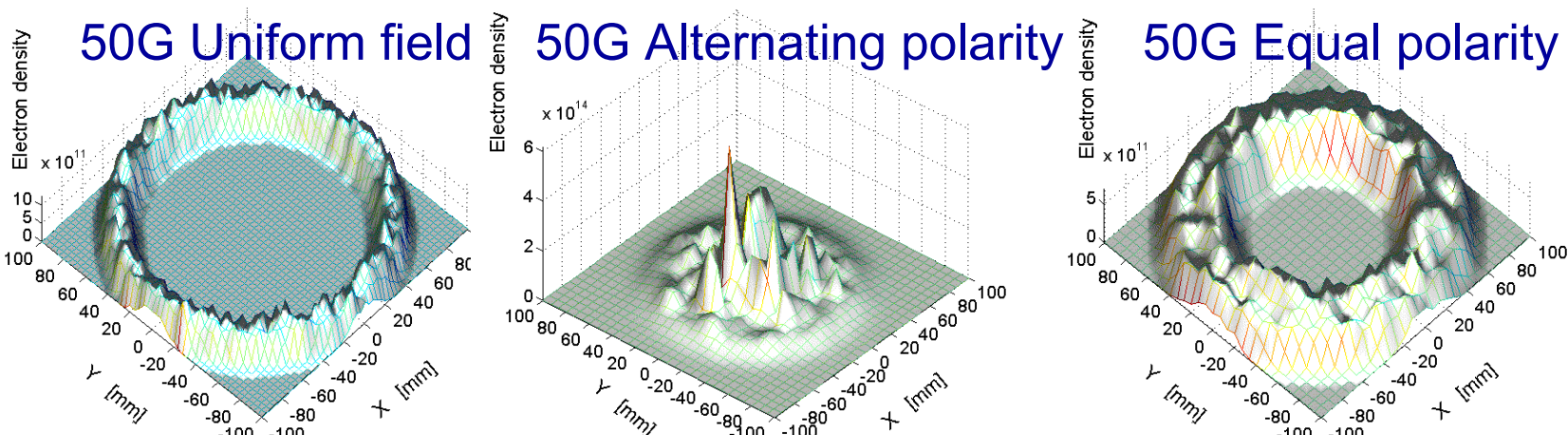
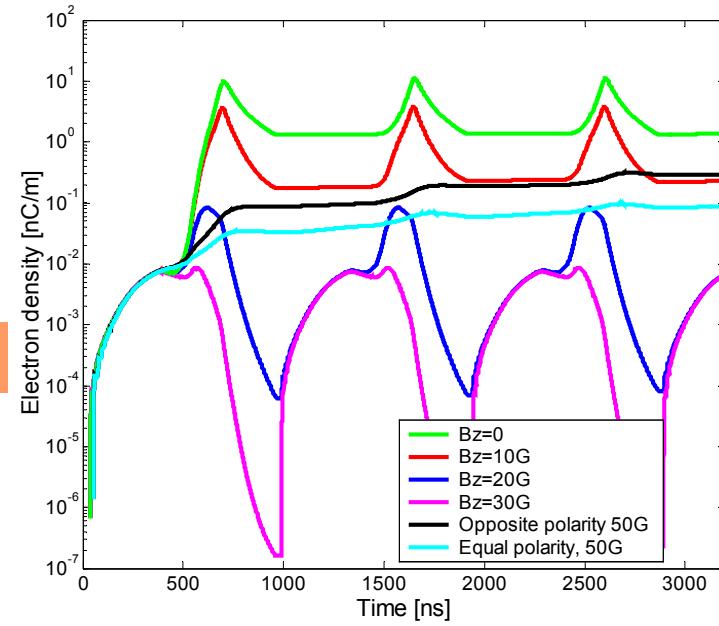
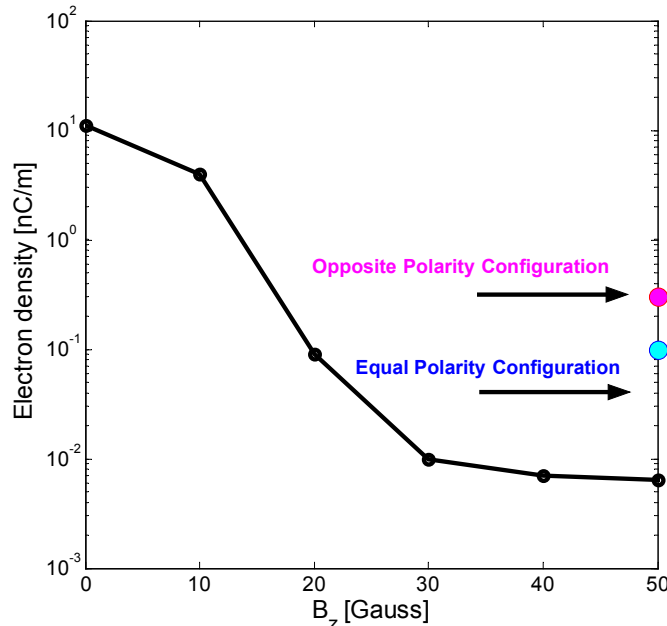
$$B_r = B_0 \frac{4ka}{\pi} \sum_{n=1,3,5}^{\infty} \sin nhk K_1(nka) I_1(nkr) \sin nkz$$

$$B_z = B_0 \frac{4ka}{\pi} \sum_{n=1,3,5}^{\infty} \sin nhk K_1(nka) I_0(nkr) \cos nkz$$

By E. Perevedentsev

$B_0 = 50$ Gauss, $h = 0.4$ m, $a = 120$ mm, $\lambda = 1$ m and 2 m

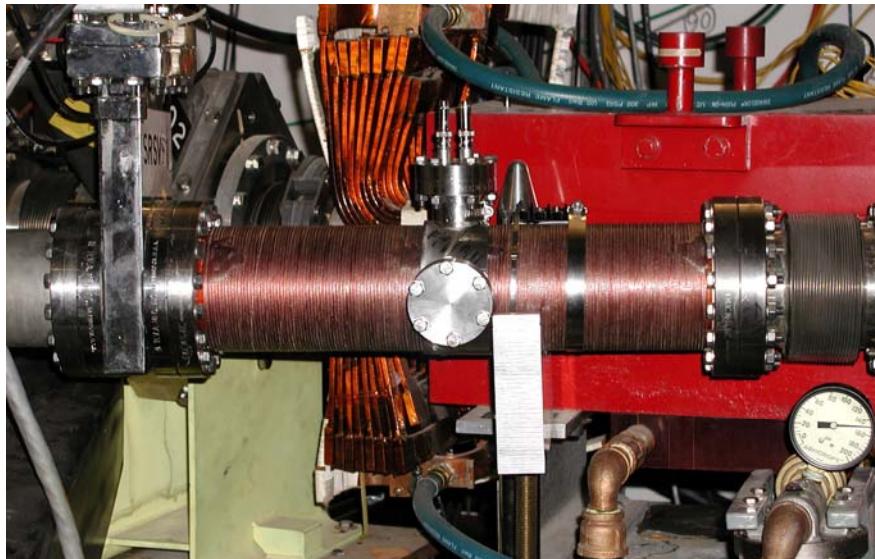
Solenoid configuration effects



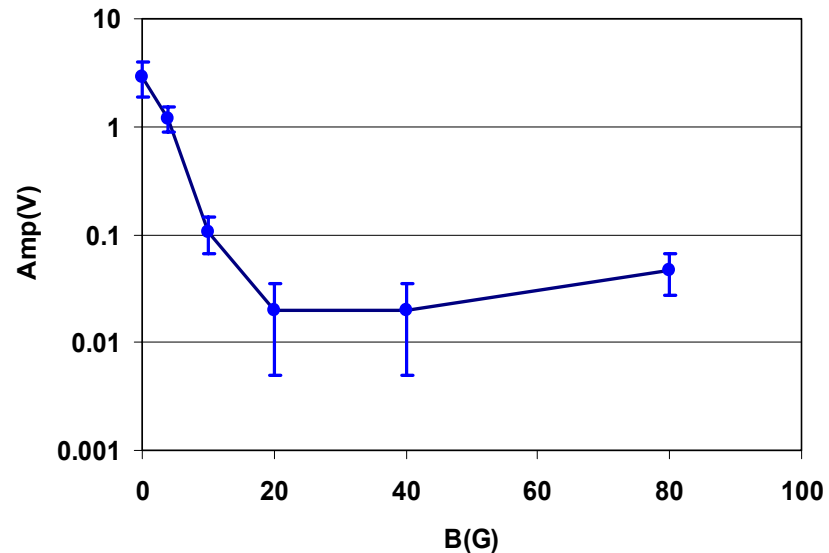
Solenoid effect -----PSR experiment



- 20G Solenoid field can reduce the e-cloud signal with a factor > 50 !

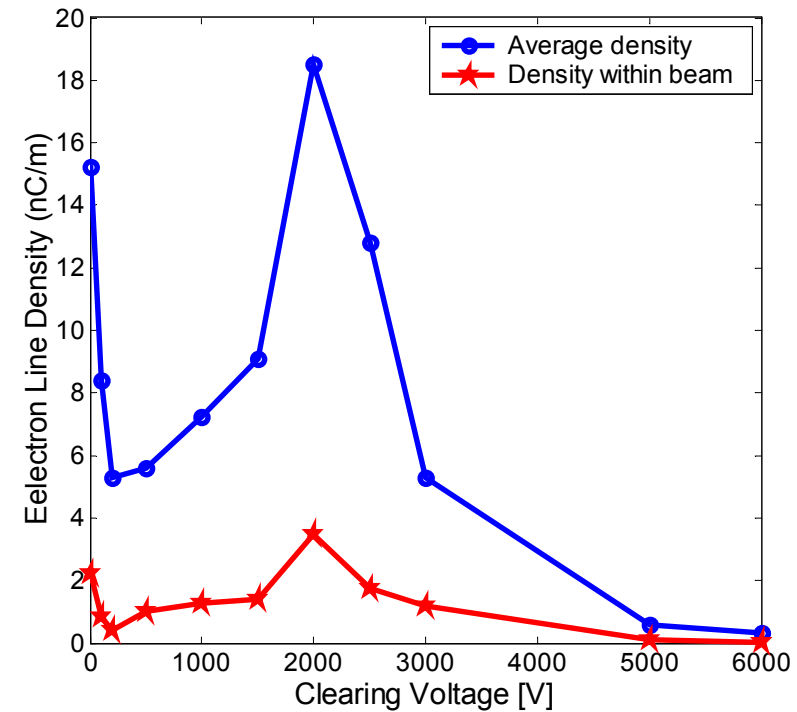
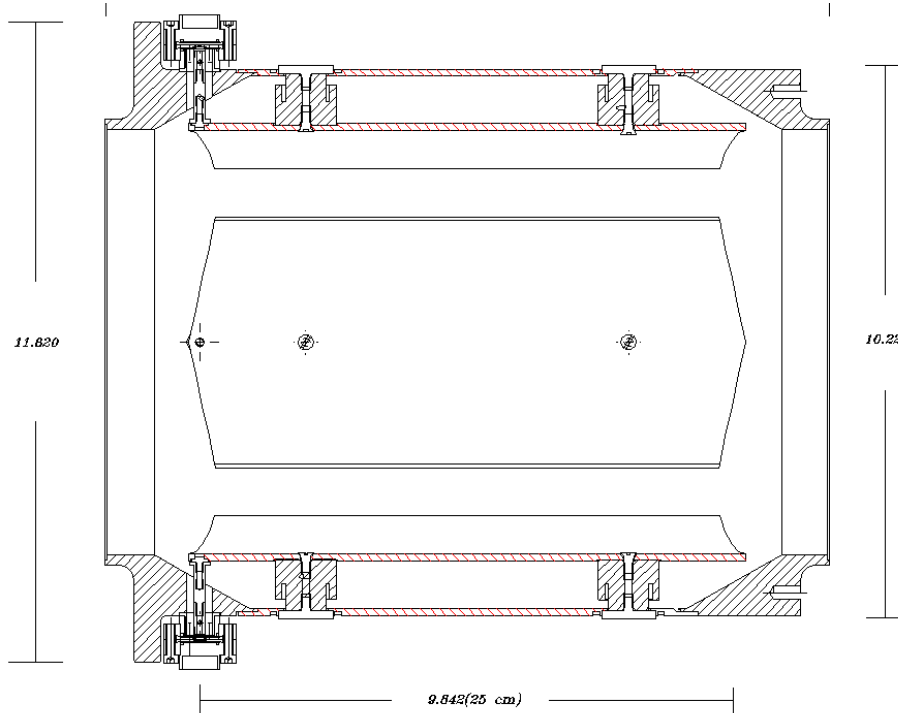


Picture of RFA (ED92Y) in a short solenoid in section 9



Effect of weak solenoid on prompt electron peak (ED92Y)

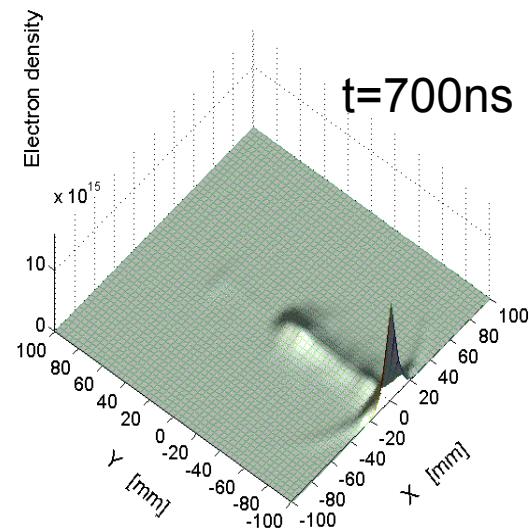
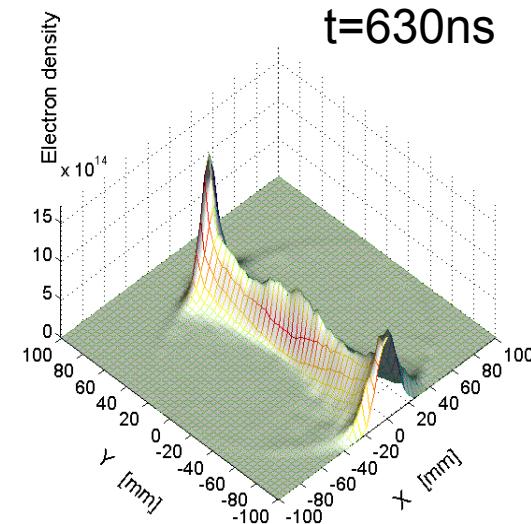
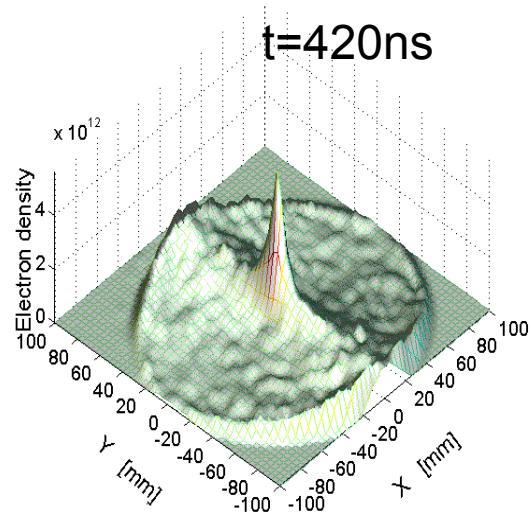
Electrode clearing effect vs. Clearing voltage (SNS Tech note 128, to be published)



e-cloud density vs. clearing fields

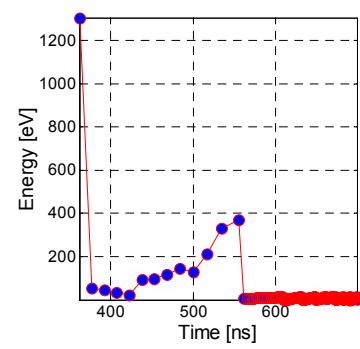
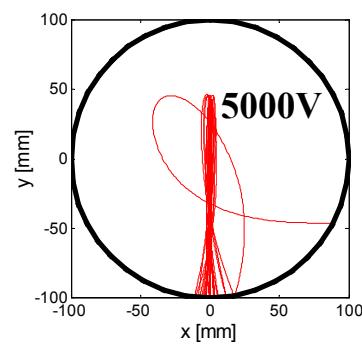
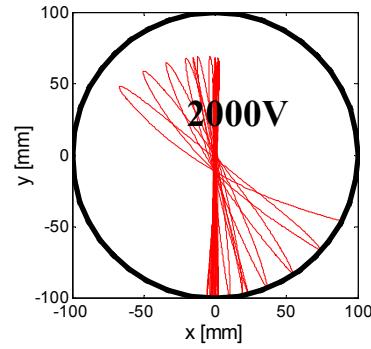
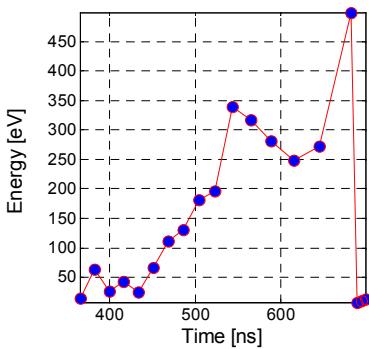
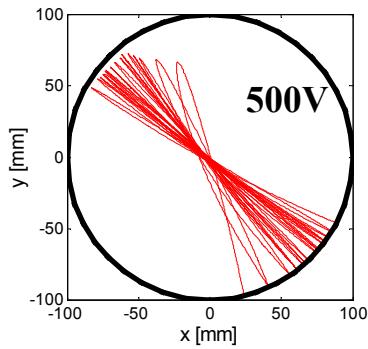
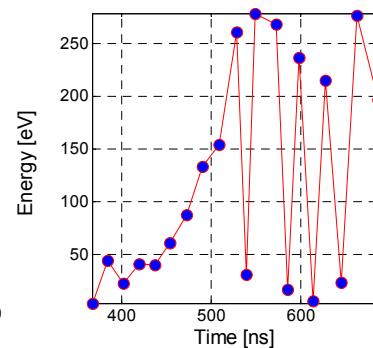
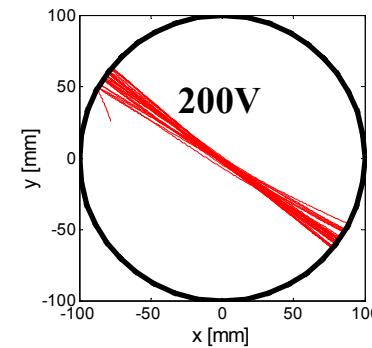
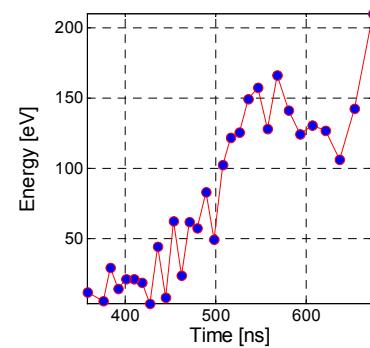
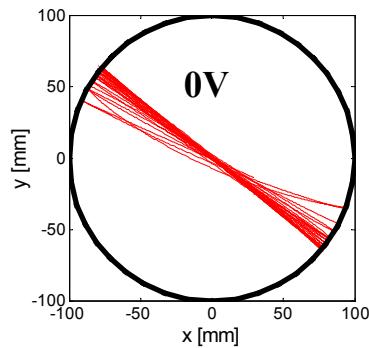
- Weak field(~200V) is very helpful
- Strong multipacting at 12kV, which could be stronger than zero field case

E-cloud distribution at different time for 500V clearing field



➤ Clearing field can cause the particle polarized toward the clearing field direction. As a result, it causes strong multipacting near the positive electrode.

Mechanism of strong multipacting due to clearing field



(BNL/SNS TECHNICAL NOTE 128, 2003)

Summary & outlook



- Electron motion under beam space charge field is investigated. (Adiabatic invariant, Nonlinear oscillation frequency, electron energy gain). Mechanism of trailing edge multipacting is clearly explained
- Many factors related to the multipacting has been investigated one by one using 3D code. The results qualitatively agree with the our analysis and experiment studies. Beam intensity, Longitudinal beam profile, transverse beam size, beam in gap are important.
- Good agreement is achieved between analysis and simulation for the multipacting in drift region and dipole magnet
- Mechanism of the clearing of e-cloud with clearing electrode and solenoid is investigated